Journal of African Earth Sciences 176 (2021) 104114

Contents lists available at ScienceDirect

Journal of African Earth Sciences

journal homepage: www.elsevier.com/locate/jafrearsci

Source rock maturity evaluation and its implications for regional petroleum charge, Sirt Basin, Libya: Insights from regional geochemical assessments and modelling study

Khaled Albriki [a,b,*], Feiyu Wang [a,b], Meijin Li [a,b], Rajab El Zaroug [c,d]

[a] College of Geoscience, China University of Petroleum (CUPB), 18 Fuxue Road, Changping, Beijing, 102200, China
[b] State Key Laboratory of Petroleum Resources and Prospecting, College of Geoscience, China University of Petroleum (CUPB), Changping, Beijing, 102200, China
[c] Geological Engineering Department, University of Tripoli, P. O. Box, 13275, Tripoli, Libya
[d] Libyan Petroleum Research Institute, P.O. Box 6431, Tripoli, Libya

ARTICLE INFO

Keywords:
Kerogen
Maturity
Source rocks
Sirt basin
Trough

ABSTRACT

Six marine and lacustrine source rocks were studied to define their thermal maturation levels in the largest, youngest, and most productive petroliferous sedimentary basin in Libya (Sirt Basin). From the oldest to the youngest, the studied source rock formations were: 1) Middle Nubian; 2) Etel; 3) Rachmat; 4) Sirte; 5) Kalash; and 6) Hagfa. The calibrated basin modelling studies (1D, 2D, and 3D) were used to generate regional maturation maps for each source rock in the basin. Thermal maturity calibration was carried out at different levels utilising measured and simulated vitrinite reflectance (VRo), pyrolysis T_{max} data, and 39 typical wells for burial history modelling and geochemical screening. Corrected bottom hole temperature data were used to obtain the geothermal gradient and heat flow throughout the basin. The thermal gradient and heat flow analyses results indicated that the Sirt Basin has an average geothermal gradient of approximately 1.58 °F/100 ft and an average heat flow of 72 m.W.m^{-2} with a systematic heat flow increase toward the basin platforms and a decrease toward the basin troughs. The conducted assessments in the Sirt Basin presented different levels of source rocks thermal maturity due to variable burial depths, with an average VRo range of 0.35%–2%. The lower Cretaceous source rocks were subjected to higher degrees of diagenesis of organic matter (i.e. mid-to over-mature rocks), with an average VRo of 0.9%–2%. In contrast, the Upper Cretaceous source rocks demonstrated a wide range of thermal maturity (from marginally to late mature) in the deepest part of the Sirt Basin (Ajdabiya trough), whereas the late Palaeocene source rocks entered the mid-to late-maturity levels in the Wadayet trough (North Ajdabiya trough).

1. Introduction

The Sirt (Sirte) Basin is the youngest rift/sag basin in north-central Libya, covering approximately 600,000 km^2 (Fig. 1). The basin was formed due to strong subsidence and block-faulting that accompanied the extensional collapse of the Sirte Arch in the late Early Cretaceous (Conant and Goudarzi, 1967; Rossi, 1991; Ahlbrandt, 2001). The subsidence of the basin reached its maximum during the Palaeocene and Eocene (Abdunaser and McCaffrey, 2014; Abadi et al., 2002). The basement and early Palaeozoic sediments of the basin subsided forming several main grabens and horsts. During the Late Cretaceous to early Cenozoic, deep troughs received significant amounts of organic-rich shales (Conant and Goudarzi, 1967; Baird et al., 1996). More than 60% of these shales interbedded with evaporites and other clastic sediments are considered to be potential source rocks that charged the discovered petroleum systems in the western, southern, central, and eastern parts of the Sirt Basin. The uplifted rift blocks, particularly their flanks and crests, served as the sites of carbonate deposition and reef development and formed the primary stratigraphic petroleum traps due to their favourable dips (Conant and Goudarzi, 1967; Goudarzi, 1980; Ameed et al., 1996; Gumati et al., 1996; Jawazi, 1996; Ambrose, 2000; Sikander et al., 2006).

The main aim of this study is to determine the thermal maturation levels and distribution of the source rocks in one of the major petroliferous sedimentary basins in Libya and Africa—Sirt Basin. The basin's known reserves constitute 43.1 billion barrels of crude oil (Ahlbrandt, 2001). From the oldest to the youngest, the Sirt Basin source rocks are: 1) the shales of the Berriasian Mid Nubian Formation; 2) organic-rich

* Corresponding author. College of Geoscience, China University of Petroleum (CUPB), 18 Fuxue Road, Changping, Beijing, 102200, China.
E-mail address: khaledalbrike@yahoo.com (K. Albriki).

https://doi.org/10.1016/j.jafrearsci.2021.104114
Received 12 November 2019; Received in revised form 2 November 2020; Accepted 13 January 2021
Available online 27 January 2021
1464-343X/

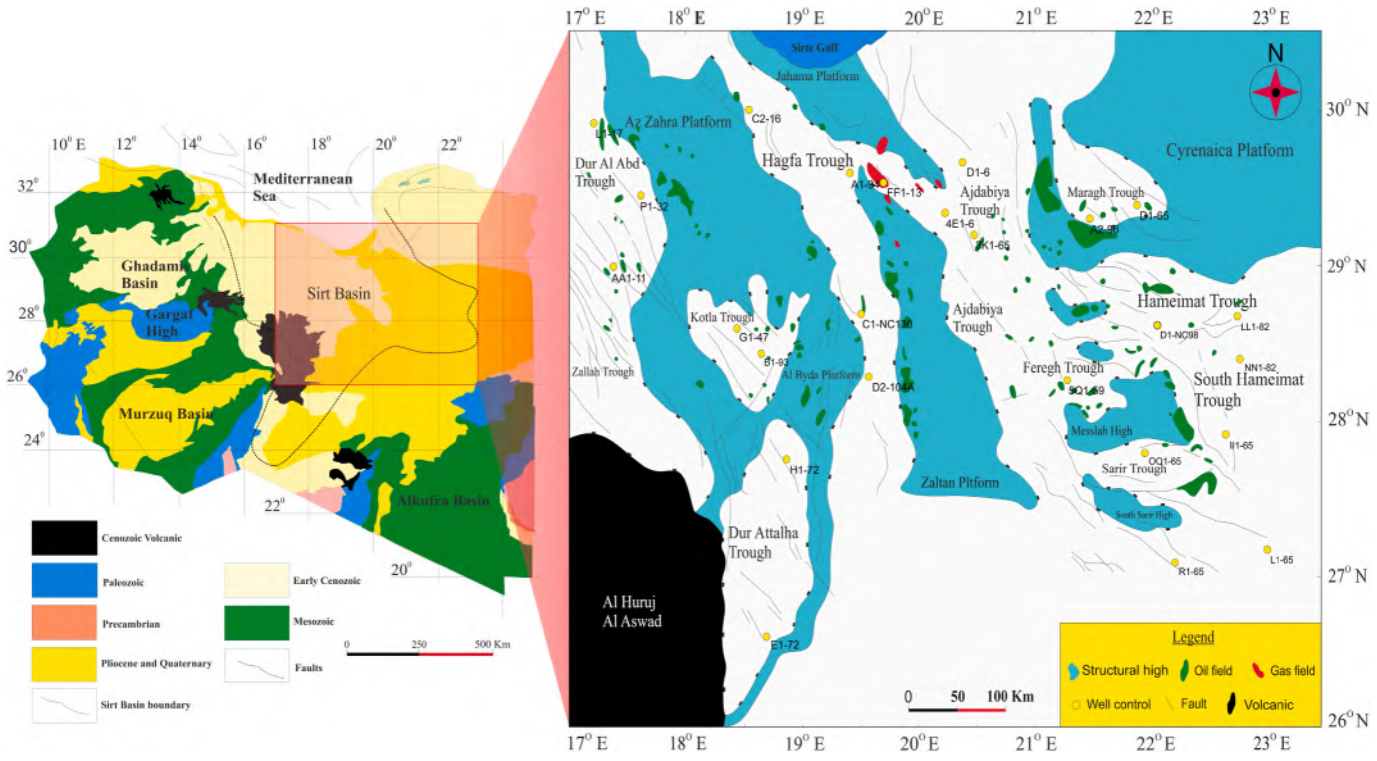

Fig. 1. Location map of the study area shows the main troughs in Sirt Basin such as Zallah and Dur Al Abd, Kotla, Dur Attalha, Ajdabiya, and eastern troughs of the Sirt Basin including Maragh, Faregh, Sarir, and Hameimat with the present-day oil and gas fields distribution. The location of the typical selected wells for the geochemical screening and 1D burial history models were marked by yellow dots (Modified from various sources).

shales of the Turonian Etel Formation; 3) shales of the Coniacian Rachmat Formation; (4) shales of the Campanian Sirte Formation; (5) argillaceous limestones of the Maastrichtian Kalash Formation; and (6) shales of the Danian Hagfa Formation. The Sirt Basin source rocks originated in seven large-scale troughs. These troughs presumably provided sufficient accommodation space and received vast amounts of fine-grained and organically rich sediments from different sedimentary environments. These organic-rich deposits subsequently became the principal source rocks that generated and charged large quantities of high-quality petroleum (Rossi et al., 1991; Hassan and Kendall, 2014). The Sirt Basin has multiple source rocks, which were identified during the early petroleum exploration and production stages by numerous local and international companies (Macgregor and Moody, 1998; Hallett, 2016). However, the thermal maturity range and geographic distribution of these source rocks have not been properly documented in the Sirt Basin due to its vast area and limited studies. The previous thermal maturation studies conducted in the basin were constrained by few datasets and lacked representative data (e.g. deep to near depocentres), especially that the assessments of source rock maturity require a properly integrated and calibrated database. For example, Gumati et al. (1991; 1996) investigated the subsidence and thermal maturity of the Upper Cretaceous and Cenozoic rocks of the Sirt Basin based on five wells. The generalised thermal maturity of the Upper Cretaceous rocks based on vitrinite reflectance (VRo) ranged 0.71–1.62%, and that of the immature Cenozoic section was determined to be 0.35–0.6%. This type of studies requires better quality and more control data to predict thermal maturity in the deeper parts of the basin with higher accuracy, where the source rocks entered their maximum thermal maturation levels.

Aboglila et al. (2010) and Aboglila and Elkhalgi (2013) carried out studies on the Cretaceous source rocks in the eastern Sirt Basin using 11 wells located in the Amal, Gialo, Nafoora, and Sarir oil fields. The study results indicated that the shales of the Rachmat, Sirte, and Mid Nubian formations reached the post-mature stages. The samples from the Sirte Formation showed maturity assortments from 0.53% to 0.85% VRo. Rachmat Formation's VRo varied between 0.90% and 1.38%, whereas the Mid Nubian Formation's VRo values ranged from 1.2% to 1.5%. Another study by El Diasty et al. (2016) analysed the Cretaceous source rocks of the Etel, Rachmat, Sirte, and Kalash formations in the western Sirt Basin and concluded that their maturity levels differed, based on the obtained VRo results: the shales of the Etel and Rachmat formations entered the mature and late-mature stages; the Sirte Formation shales presented a mid-maturity level, whereas the Kalash Formation source rock reached the early to mid-mature stages.

2. Tectonic history and basin evolution

2.1. Regional tectonic history

The Sirt Basin consists of a system of horsts and grabens that began to develop in the Late Jurassic period (Jawazi and Futyan, 1996). The basin structure evolved as a rifted margin of an embayment on the northern African Plate, following a sequence of tectonic events that led to the breakup of the supercontinent Pangea. These tectonic events caused rift development along the present northwestern margin of the African continent from the Middle Triassic onwards. Crustal separation and seafloor spreading commenced in the Early Jurassic, creating the central Atlantic Ocean between northwest Africa and North America, and were followed by the opening of the central Tethyan Basin during the Middle Jurassic (Gumati and Schamel, 1988; Gumati et al., 1996; Sikander and Basu, 2006).

The Early Cretaceous rifting in the Sirt Basin occurred as a response to the extensional forces generated along the zones of crustal weaknesses between the two African crustal blocks. This rifting led to the collapse of the preexisting Sirte Arch (NE–SW positive structural feature). The following early rifting phase was characterised by the onset of late rhyolitic and basaltic volcanism, where the granites were dated to approximately 150 Ma and the basic to intermediate volcanic rocks were

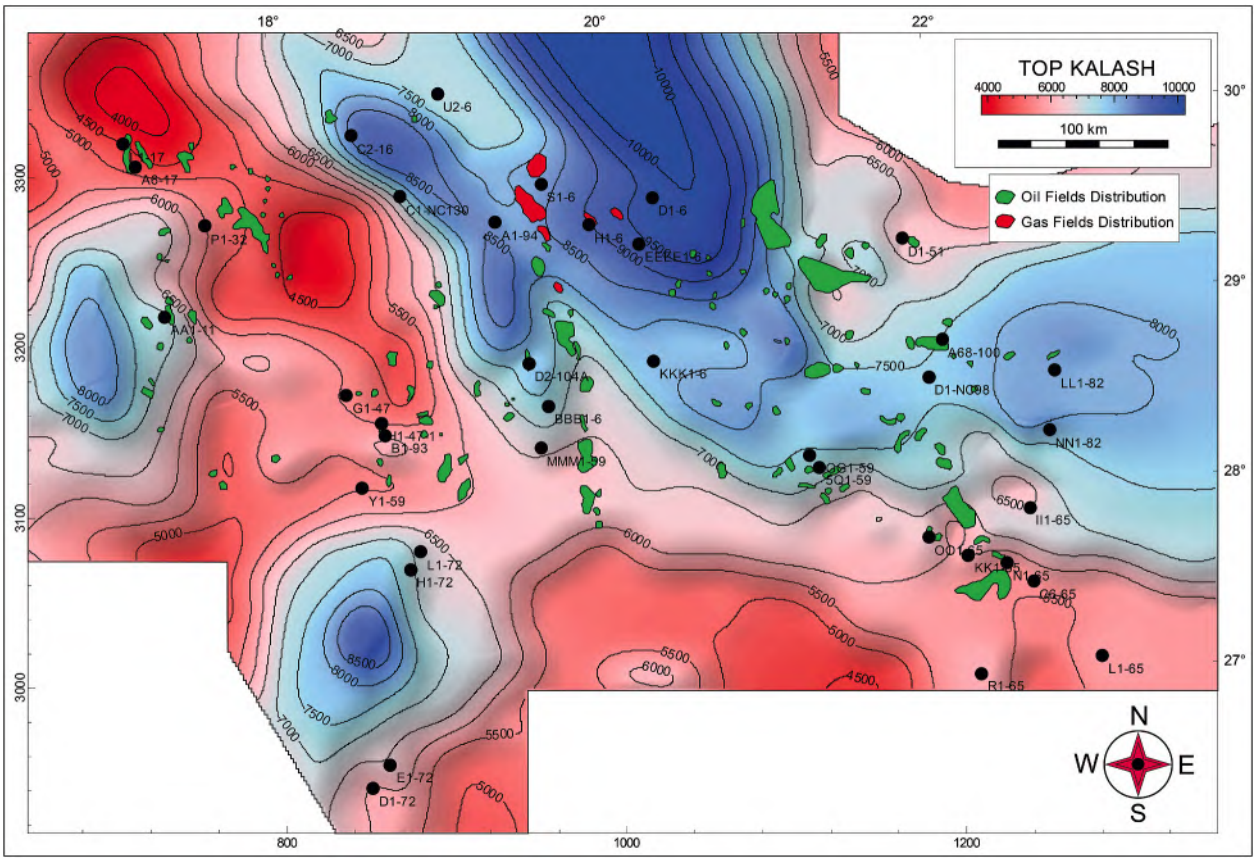

Fig. 2. Present-day structural features (NW–SE), oil and gas fields distribution, basin structural highs (platforms), and structural low (troughs) in the Sirt Basin based on the top of the Kalash Formation. A total of 39 wells were selected for geochemical screening (black dots) and calibration to reconstruct a 1D burial history model (Genesis project) using Trinity software. The LLNL model was utilised for further source maturity estimations and the corrections of 2D simulated maturity maps (compiled from various sources using multi correlation gridding vs dense Formation tops from well control data).

dated to approximately 130 Ma (Hallett, 2002; Abdulbaset et al., 2008). In the Late Cretaceous, active subsidence occurred, which slowed down with time. The Palaeocene and early Eocene were characterised by slow subsidence and extensional fault reactivation as a response to the relative motion of the American, African, and Eurasian plates during the opening of the Atlantic Ocean and the development of the Tethys Basin at the foreland edge of the African Plate (Anketell, 1996; Guiraud and Bosworth, 1997; Ziegler and Roure, 1999; Sikander and Basu, 2000).

The structural configuration of the Sirt Basin controlled the generation, expulsion, migration, and trapping of a large amount of hydrocarbons (Fig. 2). The maturity of the Sirt Basin source rocks was apparently influenced by the sedimentary basin formation, type of the accumulated sediments, their distribution, geothermal gradient, heat conductivity, and heat flow patterns. These factors are crucial for understanding the thermal maturation history of the source rocks to better evaluate the amount of hydrocarbons that charged the explored and unexplored oil and gas traps. The organic-rich source rocks in the Sirt Basin were predominantly deposited in the rapidly subsiding fault-bounded troughs in the Triassic, Cretaceous, and lower Palaeocene. The Campanian source rocks are the most widespread and generated the majority of discovered hydrocarbon plays in the Sirt Basin (Ghori and Mohammed, 1996; Ahlbrandt, 2001). The petroleum migration happened laterally and vertically through the boundary faults (Rift faults), followed by vertical and lateral migration along the fault fractures and, finally, the hydrocarbons were trapped in reservoirs by vertically sealed faults on the platform shoulders. Secondary petroleum migration toward the platform areas occurred due to later tectonic activity (Gumati and Nairn, 1991; Anketell, 1996; El Ghoul, 1996; Roohi, 1996; Ahlbrandt, 2001; Abdunaser and Mccaffrey, 2015; Hallett, 2016). The past and present exploration efforts have been concentrated on the structural highs of the Sirt Basin (Hallett and El Ghoul, 1996; Rusk, 2001), and not enough attention has been paid to the troughs, where, we expect the future petroleum discoveries in the Sirt Basin.

The most significant tectonic event in the Sirt Basin occurred when the NE–SW-oriented Sirte Arch collapsed and initiated the development of the Mes-Cenozoic petroleum system by developing structural lows. These lows or troughs received and preserved sufficient amounts of high-quality organic matter between the Early Cretaceous and late Palaeocene, forming potential source rocks (El-Alami et al., 1989; El-Alami, 1996; Sikander and Basu, 2000). The Lower to Upper Cretaceous source rocks are the dominant ones in the Sirt Basin and are represented by the lacustrine and marine early rift shales (e.g. Mid Nubian Shale). The late Palaeocene shales (e.g. Hagfa Formation) are low-quality source rocks likely due to the low rates of organic matter supply or low intensity of the preservation conditions. However, the Mesozoic rifting in the Sirt Basin also promoted the development of several good structural traps, as well as a few combined hydrocarbon traps (stratigraphic and structural).

2.2. Regional stratigraphy

The Sirt Basin is characterised by several large-scale troughs separated by structural highs (generally, carbonate platforms) oriented in the NW–SE direction. The present-day basin architecture is dominated by elongated structures (Fig. 2), which are interpreted to be formed during intracontinental rifting and collapse events during the Early to Late Cretaceous. Such elongated structures are considered typical of the Tethyan (Mediterranean Sea) rift system, which began active rifting in

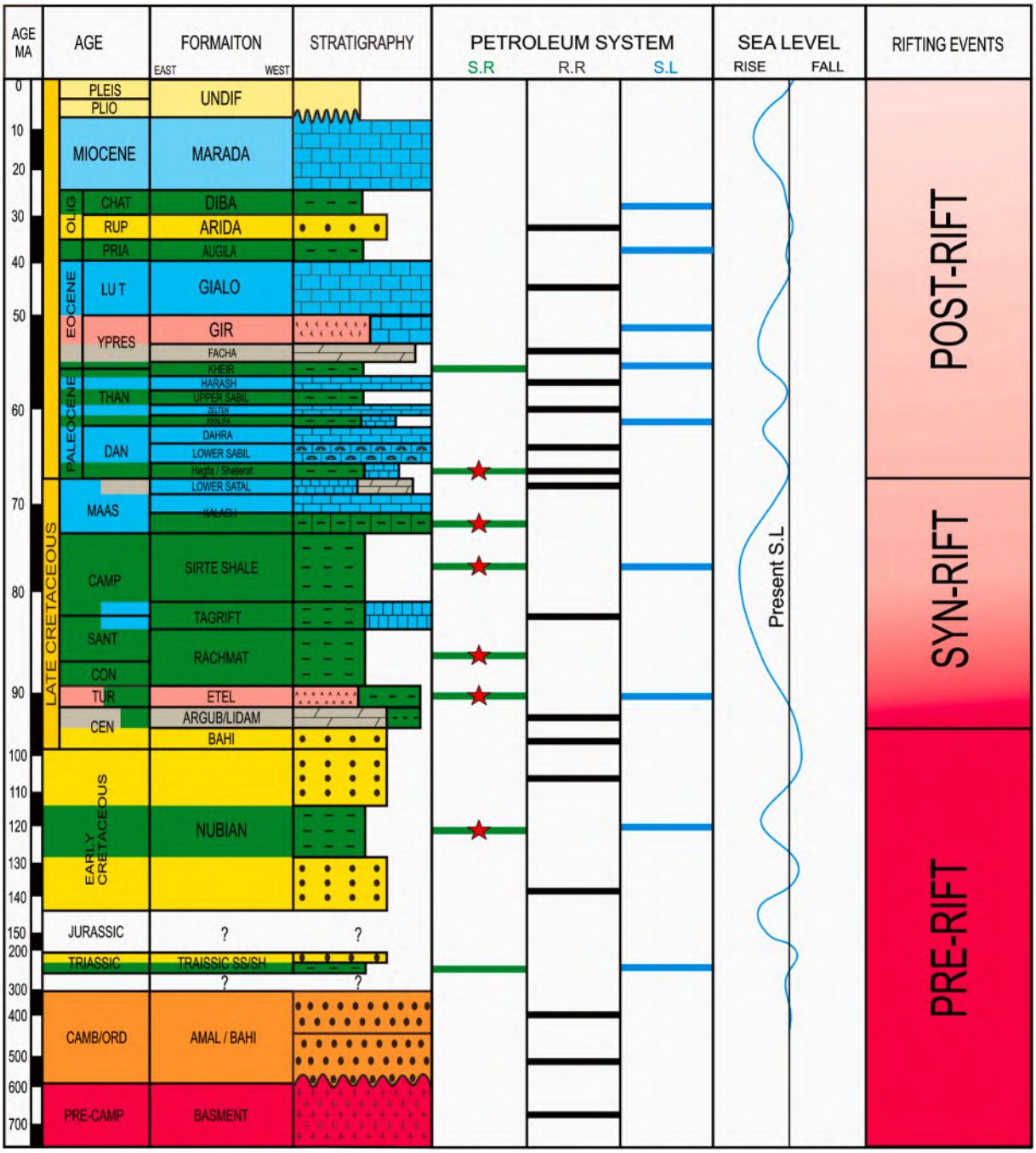

Fig. 3. Generalised stratigraphic column of the Sirt Basin showing the main stratigraphic units, including the studied source rock intervals (marked with red stars), petroleum systems (S.R, R.R, and S.L refer to the source rock, reservoir rock, and seal rock, respectively), significant sea-level changes, and the major rifting events (the rift stage boundaries are denoted according to Harding, 1984) that shaped the basin to the present-day structural style (modified from various sources).

the Early Cretaceous and peaked in the Late Cretaceous (Goudarzi, 1980; Wennekers et al., 1993; Klemme, 1994; Gumati et al., 1996; Roohi, 1996; Hassan et al., 2014). Harding (1984) provided a general overview of the Sirt Basin depositional history based on three primary rifting cycles:

1) Pre-rift (~740–98 Ma): The depositional system of the pre-rifting phase was characterised by the sediments deposited during the initial crustal stretching, when thick successions of sandstones (i.e. the Amal, Bahi, and Nubian formations) were accumulated in the area. These sandstones represent the primary reservoirs in the eastern Sirt Basin (e.g. the Sarir oil field) and were charged from the Jurassic and Cretaceous source rocks (Fig. 3).
2) Syn-rift (~98–66 Ma): The syn-rift cycle started with the deposition of sandstones (e.g. the Bahia and Nubian formations) and continued with a widespread early Cenomanian to late Maastrichtian (~98–66 Ma) transgression when thick successions of carbonate and shale were deposited in the marine environment. The transgression was followed by a rapid sea-level fall and erosion of the high-relief topography left at the end of the syn-rift phase. The continued tectonic activity led to the development of several shallow basins during the Turonian (~90 Ma) when most of the evaporites were deposited in the basin. The marine transgression reached its maximum during

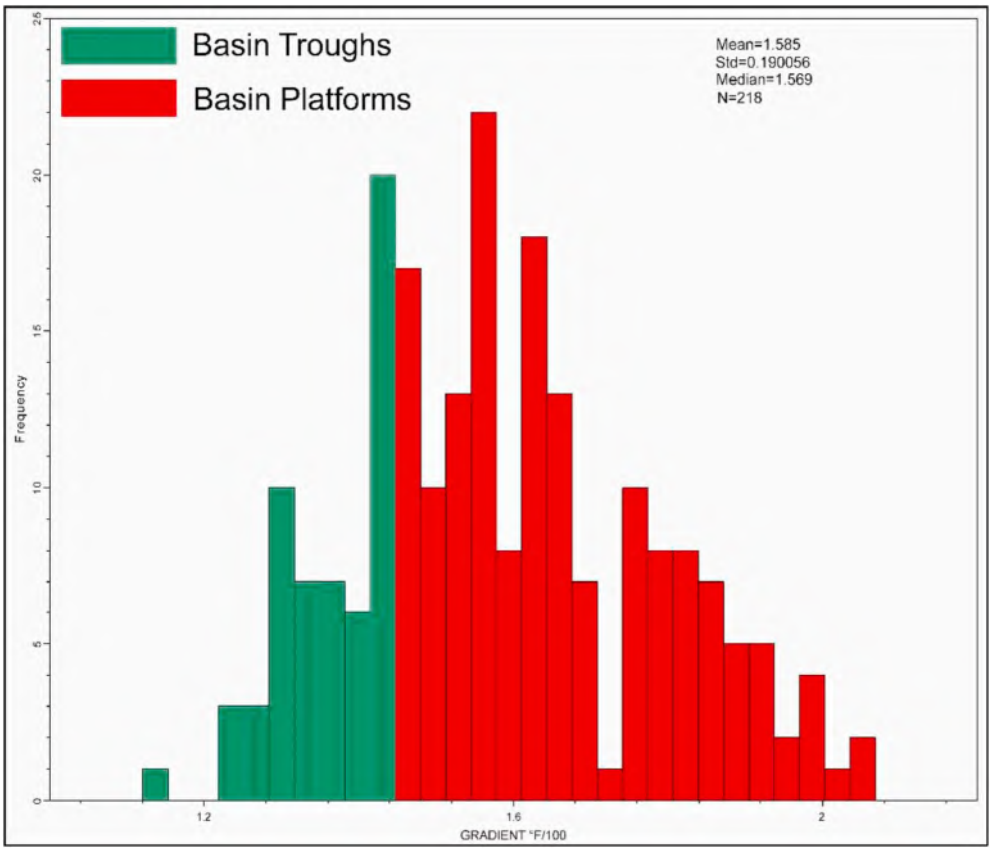

Fig. 4. Geothermal gradient distribution in the Sirt Basin. An average gradient was determined to be 1.56 °F/100 ft.

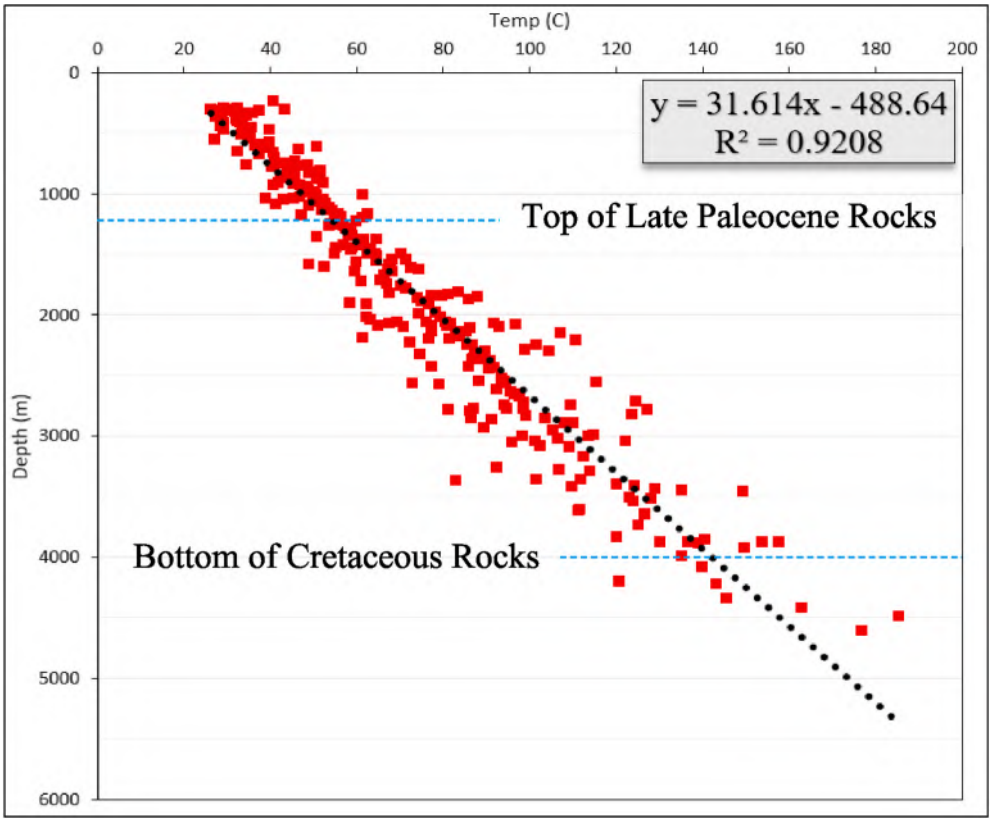

Fig. 5. Temperature–depth relationships as per the 232 corrected bottom hole temperature (BHT) measurements at a surface temperature of 20 °C calculated in Trinity software (T3) to calibrate the geothermal gradient for further maturity assessments of each source rock.

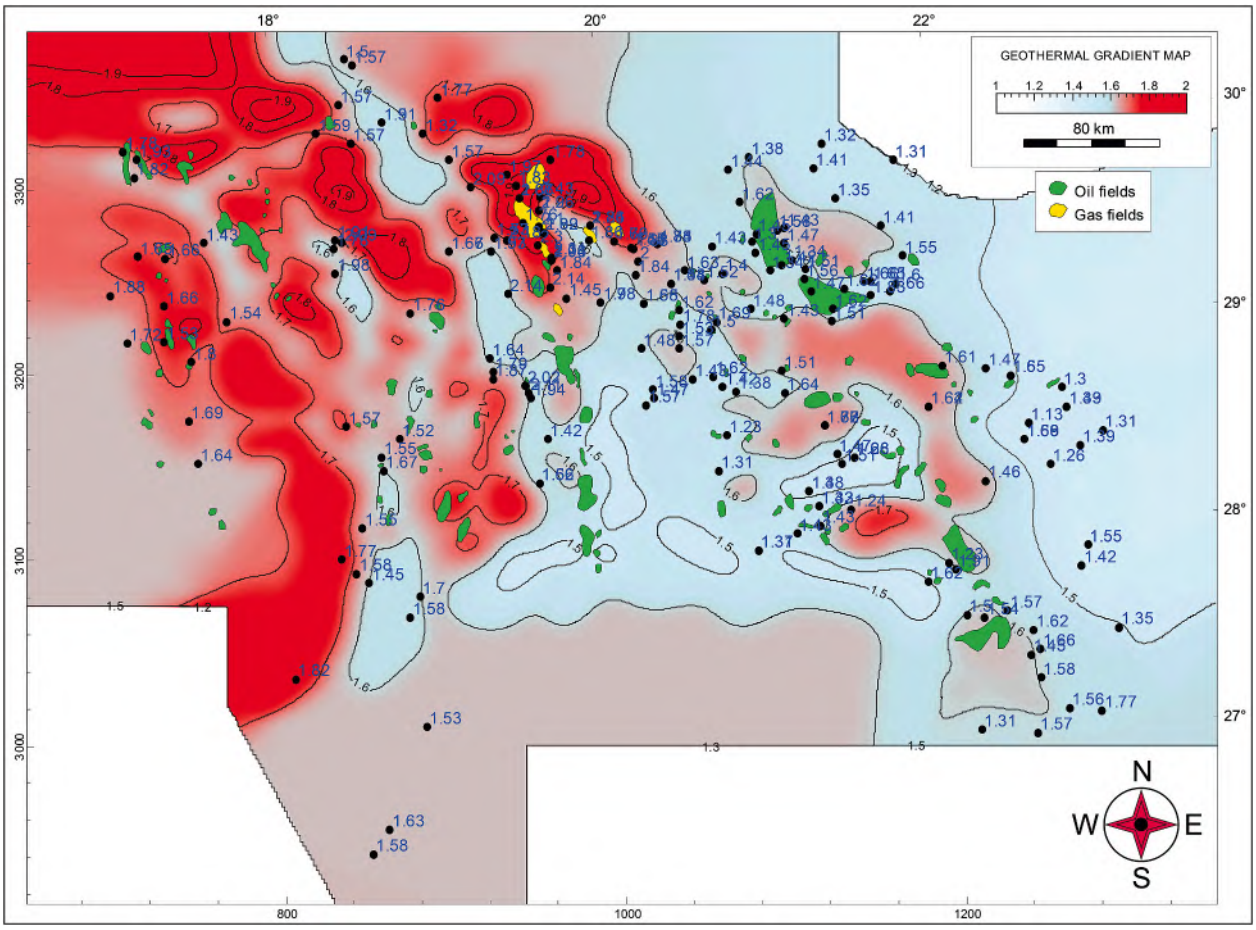

Fig. 6. Present-day geothermal gradient map of the Sirt Basin.

the Maastrichtian (~71.1 Ma) with the deposition of the Rachmat Formation. Therefore, the syn-rift phase was the most prolific in terms of organic-rich deposits, when the primary source rocks of the Sirt Basin were deposited.

3) Post-rift (~68 Ma–Present): The post-rift phase is represented by the Palaeocene deposits, which contain approximately one-third of the discovered hydrocarbons in the Sirt Basin. The Palaeocene deposits are predominated by carbonate and shale lithologies. The troughs were filled with marine shales having thin shaly limestones. During the Eocene (~56–40 Ma), a variety of environments existed in the area, and the Gialo and Gir formations were deposited. They are typified by deep-water shales, shallow-water carbonates, and evaporates. During the Eocene, the carbonate factory was active and resulted in the deposition of carbonates with variable thicknesses. Carbonate accumulation was controlled by the available accommodation space and depositional environment. The Miocene (~23–5 Ma) deposits presently outcrop over large areas in the western Sirt Basin and constitute thick limestone deposits (e.g. the Marada Formation). The Oligocene deposits of marine origin are restricted to the northeast Sirt Basin, whereas non-marine rocks proliferate in the southwest Sirt Basin, toward the basin margin. In the post-Miocene times, the Sirt Basin experienced an extraordinary event, with a significant drop in the sea level during the Messinian (~6 Ma). Generally, the stratigraphic fill of the Sirt Basin is complex and has not been well defined owing to many reasons, such as large area, complex local geology, and the lack of accurate regional age dating. To date, most studies in the basin have been accomplished in small areas, and local observations have not been integrated across the basin scale.

3. Methodology, calibration, and data origin

Thermal maturity in this study was determined by measured optical and simulated vitrinite reflectance (VRo) from the Lawrence Livermore National Laboratory (LLNL) and Arco models calibrated against the 1D burial history models and pyrolysis T_{max} data. We utilised the bottom hole temperature (BHT) data from 232 wells to map the present-day geothermal gradient and heat flow regime throughout the Sirt Basin. We also used the heat flow and geothermal data to calibrate and generate five regional thermal maturity maps by Trinity (T3) software (ZetaWare, Inc). Thirty-nine typical wells were selected for further geochemical screening and conducting a 1D calibrated burial history modelling study. The entire area of the Sirt Basin was divided into seven large-scale troughs for detailed thermal maturity evaluations to discriminate between the source rocks due to their possible lateral heterogeneity and obtain accurate maturity trends vs the burial depth using the calibrated 1D and 2D modelling approaches. This study is predominantly based on the data collected from the internal technical reports of various oil companies. The permission to use this technical information was given via personal communication. We also utilised the data from several published papers with authorisation for their further use, textbooks, and other unpublished work, such as internal company reports. The information on the drilled wells, basin stratigraphy, and BHT was obtained from various published and unpublished sources and digitised.

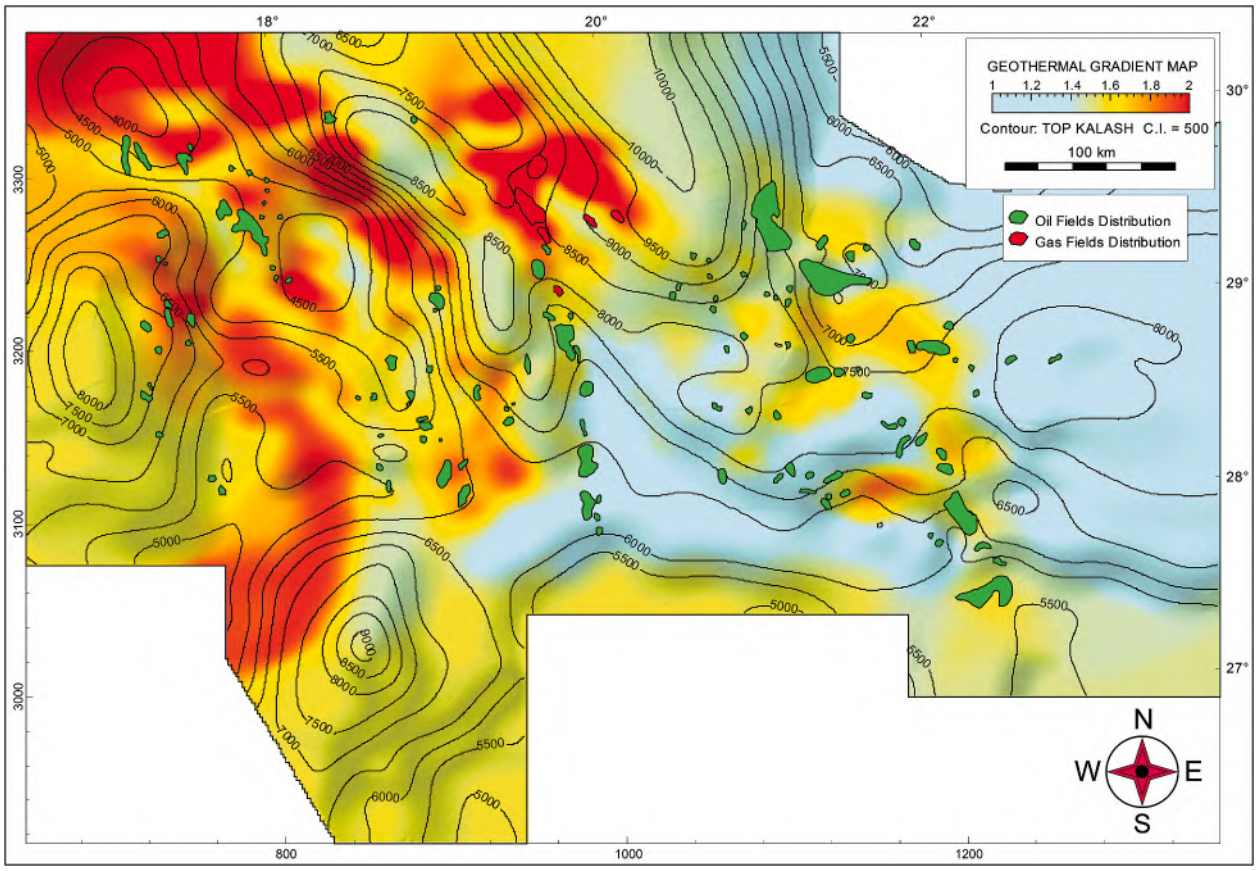

Fig. 7. Calibration of the thermal gradient data with the top of the Kalash Formation. This calibration provides descriptions and an appropriate explanation for the thermal gradient anomalies and their distribution within the troughs and on the platforms of the Sirt Basin.

4. Results and discussion

4.1. Regional thermal regime evaluation

4.1.1. Geothermal gradient analysis

Sedimentary-basin subsidence causes thermal maturation in the progressively buried sedimentary layers (Cornford, 1998). The continental crust palaeo temperatures within the sedimentary basin-fill are controlled by the basal heat flow history and 'internal' factors, such as the variations in thermal conductivity and heat generation from radioactive sources. It is critical to analyse the geothermal gradient, heat flow, and heat production to understand their impact on the source rock maturity, oil and gas maturity, and sedimentary basins due to the thermal blanketing effect of sediments (McKenzie, 1981; Ungerer, 1990; Horsfield, 1994; Waples, 1994; Pepper and Corvi, 1995; Allen and Allen, 2013). The thermal gradient distribution in the Sirt basin seems to be controlled by seven large-scale troughs (Fig. 2) and their thick sedimentary fills of fine-grained material.

We plotted the BHT data from 232 wells vs the burial depth using a linear regression equation ($y = ax + c$) and a 0.92 correlation factor. We then calculated the slope of the line to define the geothermal gradient of Sirt Basin. The resultant average thermal gradient was determined to be approximately 1.56 °F/100 ft. Figs. 4 and 5 present the distribution of the calculated thermal gradient, showing its highest and lowest values. Mapping and calibration of the thermal gradient superimposed on the top of the Kalash Formation revealed that the thermal gradient was lower in the troughs than on the platforms. We suggest that this might be associated with the lithology of the rocks present in these troughs (i.e. shales and marls), which differs from that of the carbonate platforms (i.e. carbonates and anhydride). More permeable rocks (carbonates and anhydride) can better conduct and distribute heat rather than the fine-grained, non-permeable rocks (shales, marls) present in the troughs. The higher geothermal gradients modelled for the western Sirt Basin, especially that for the Az Zahra-Hufra platform, are likely related to such structural relationships. In contrast, higher geothermal gradients observed near the Wadayet trough seem to be associated with the basement highs only (Fig. 6–Fig. 7).

4.1.2. Heat flow analysis

The analyses of the heat flow regime and heat production patterns in the Sirt Basin were carried out using 66 and 24 measurements for the heat flow and heat production, respectively, from the wells located in the troughs and on the platforms. Data analysis and interpretation indicated that heat flow was elevated as a response to the tectonic movements, such as the Mesozoic rifting during the Cretaceous rift phase (~98–66 Ma). The conductivity analysis showed that conductivity generally ranged between 2 and 2.1 $w.m^{-1}.k^{-1}$ (Fig. 8), with higher conductivity in more porous rocks (e.g. sandstones, carbonates). In contrast, soft and less porous materials (e.g. shales) demonstrated low conductivity. Heat flow increased toward the northwest Sirt Basin. The heat flow trends in the Sirt Basin are similar to the geothermal gradient trends, with the highest heat flow present on the basin platforms rather than in the basin troughs.

The average heat flow was calculated to be 72 $m.W.m^{-2}$, whereas heat production averaged 3.9 $\mu W\ m^{-3}$ (Fig. 9). The heat flow is distributed quite uniformly throughout the basin, showing a systematic increase and decrease from the basin platform toward the troughs. The heat flow on the platforms is higher than that in the troughs. This discrepancy is probably related to the heat refraction pattern associated with the basin-wide fault block structures or considerable input of fine-grained sediments in the troughs compared with the platforms. The average heat flow calculated for the Sirt Basin is lower than that in the

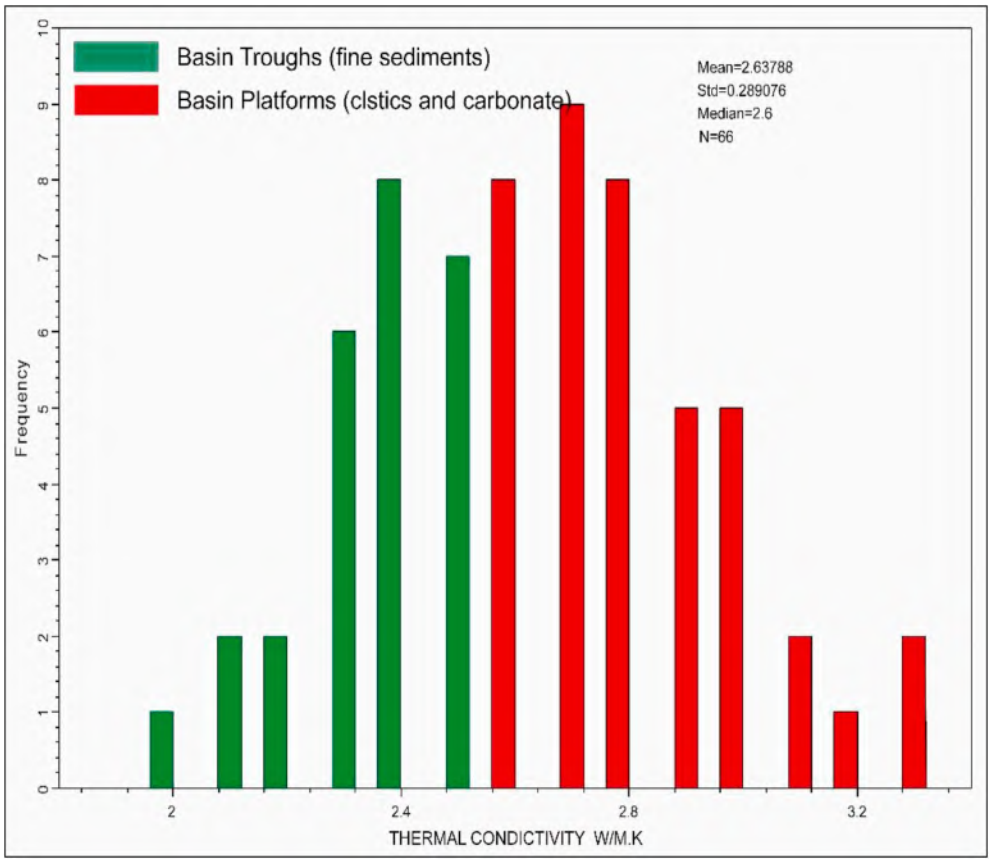

Fig. 8. Distribution of the thermal conductivity with an average of 2.6 w/m.k. The rocks with higher conductivity are located on the basin platforms.

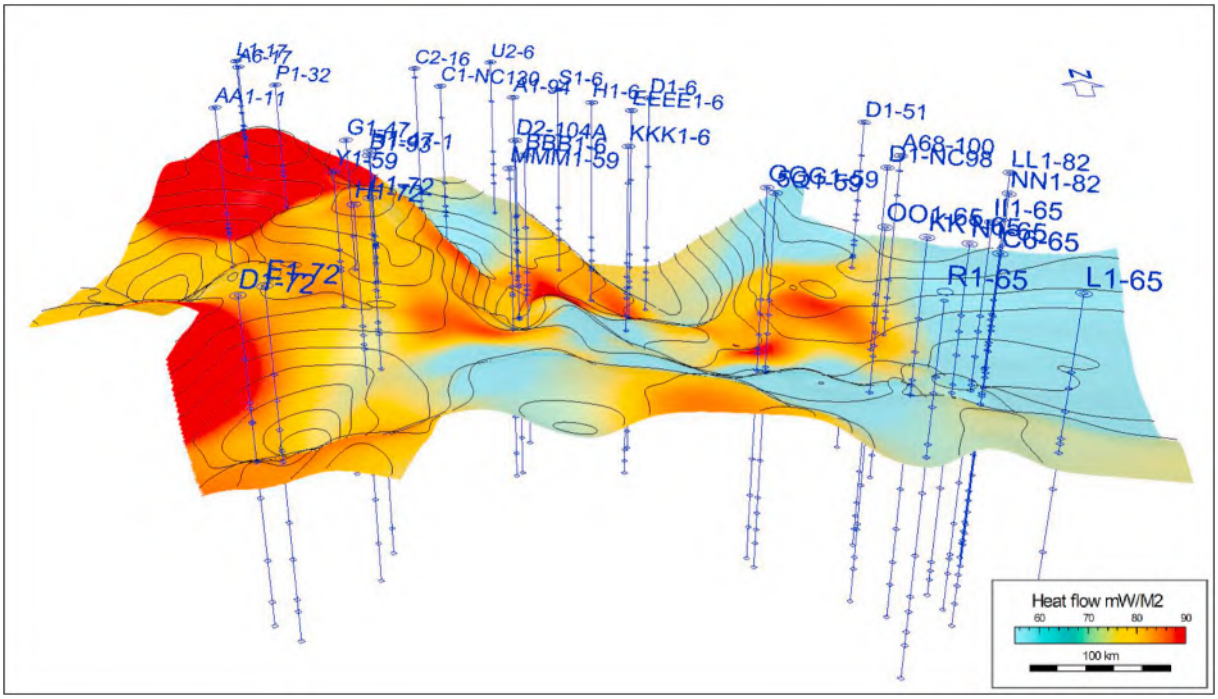

Fig. 9. Heat flow distribution model of the Sirt Basin. The top of the Kalash Formation was used for depth calibration purposes. The 1D burial history models based on 40 wells were applied to calibrate the 1D heat flow models using Genesis software for further corrections and better extrapolation results.

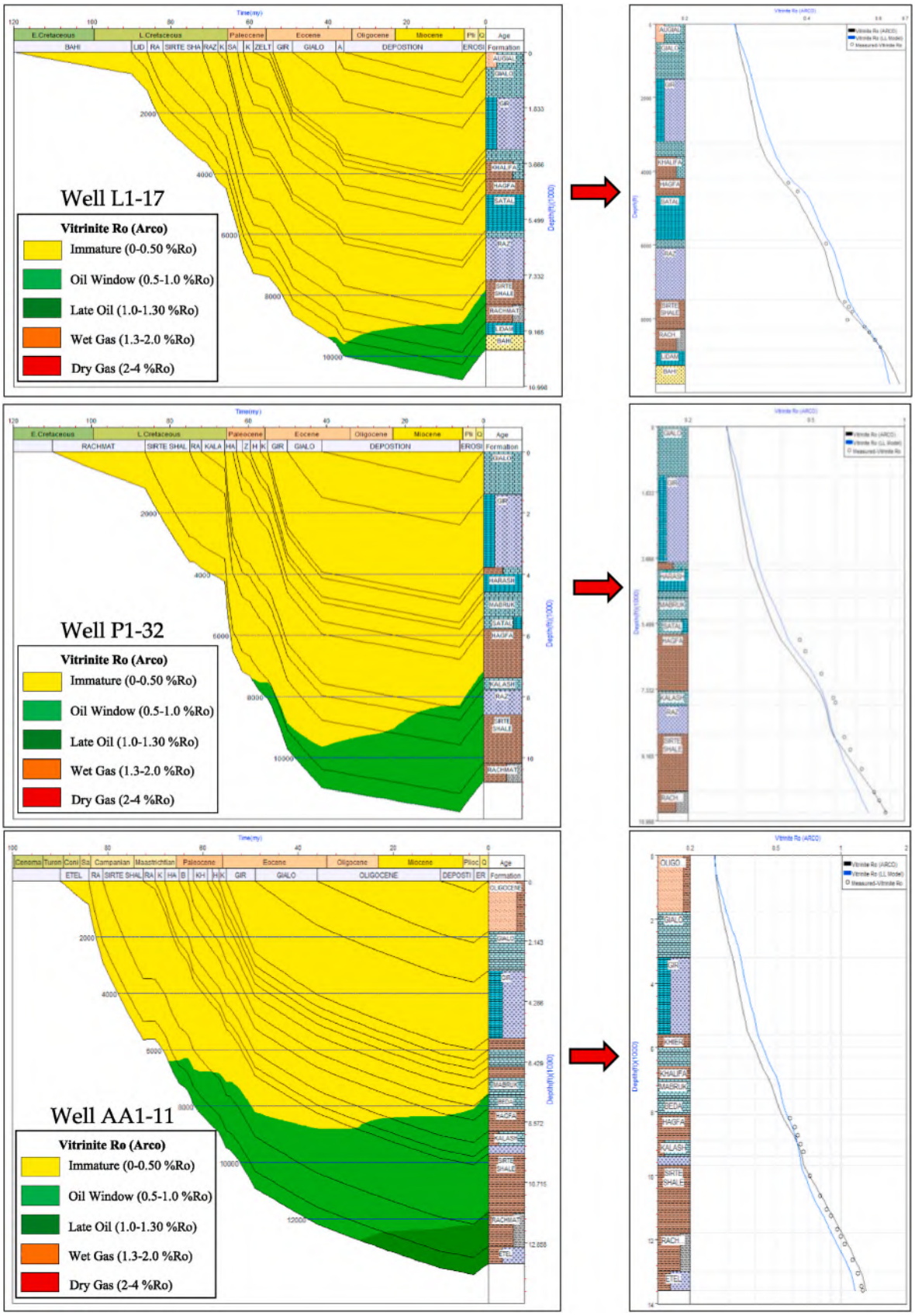

Fig. 10. Thermal maturity levels in the Zallah and Dur Al Abd trough estimated using the 1D burial history models calibrated against the VRo data from three selected wells (L1-17, P1-32, and AA1-11). The model data input and output were accomplished using Genesis software.

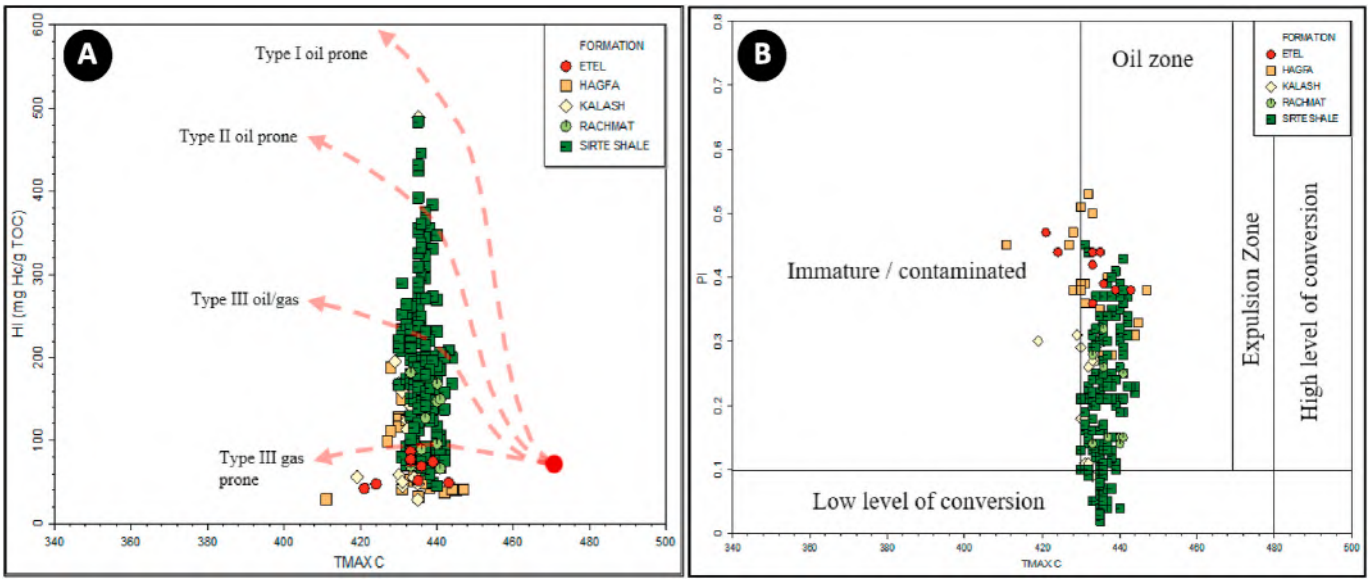

Fig. 11. Pyrolysis T_{max} data vs the hydrogen (A) and production indices (B) from the three selected wells (L1-17, P1-32, and AA1-11) in the Zallah and Dur Al Abd trough.

Sahara Basin in Algeria (80–120 m.W.m^{-2}) or in the Red Sea region (75–100 m.W.m^{-2}), which may be the result of the Cenozoic tectonic activity in the Red Sea rift (Nyblade et al., 1996).

4.2. Areal maturity modelling and analysis

4.2.1. Zallah–Dur Al Abd trough

Thermal maturity in the Zallah–Dur Al Abd trough was evaluated using three typical wells (L1-17, P1-32, and AA1-11, see Fig. 1) and four source rocks (i.e. shales of the Rachmat, Sirte, Kalash, and Hagfa formations). The burial history models in this part of the basin were constructed using the calibrated Arco technique and 1D Genesis Zetaware basin modelling software. The source rock origin, distribution, quality, type of organofacies, lateral and vertical variations at a local scale, and maturity levels were not well documented in this area, except the study done by the Robertson Research Group (1989) for the Upper Cretaceous section. They concluded that the Sirte shale attained mid-maturity levels with a VRo ranging from 0.7% to 0.8% (wells A1-17, L1-17, A6-17, P1-32, Z1-11, and Q1-11). The Sirte shale maturity increased toward the trough depocenter and exceeded 0.85% VRo (wells AA1-11, G1-11, and OO1-11). The Rachmat Formation was determined to enter mid-to late-maturity levels with a VRo of over 0.95%.

Our results indicated that the Rachmat Formation entered a late-maturity level in the early Oligocene (~33 Ma), as indicated by well AA1-11. This well is located near the Zallah–Dur Al Abd trough depocenter, where the maximum maturity levels likely occur (Fig. 10). Due to the lack of data in the vicinity of the depocenter, we utilised well AA1-11, as the nearest one to the depocenter, to compensate for this shortcoming. Well AA1-11 is the ideal selected well to analyse the maturity levels of all four targeted source rocks. The source rocks reached the maximum burial depth in the late Pliocene (~5 Ma), followed by an uplift that has continued to the present day. However, the Cretaceous section entered the mid-maturity window in the early Pliocene (~70 Ma), whereas the present-day subsidence levels allowed the source rocks to enter the late-maturity window, indicating that the Cretaceous source rocks reached a thermal maturity level high enough to generate commercial amounts of hydrocarbons.

Thin marine shales of the Campanian Sirte Formation are widely distributed on the platforms of the Sirt Basin, and their thickness can exceed 1500 ft (457.3 m) in the deepest part of the basin (Ajdabiya trough). This marine source rock contains type I/II kerogen and has a mid-maturity level, as indicated in this study, with an average VRo of 0.72%. The other two source rocks in this trough, the Kalash and Hagfa formations, are less significant than the Sirte Formation for hydrocarbon generation due to their low maturity levels (early maturity) and low total organic carbon (<1.5 %TOC) values. The three selected wells (L1-17, P1-32, and AA1-11) indicated a systematic increase in the maturity levels toward the trough depocenter and a systematic decrease toward the adjacent structural highs (i.e. platforms). However, we deem that the source rocks of the Kalash and Hagfa formations need further analysis of kerogen kinetics to better understand their kerogen transformation ratios (% TR) and the timing of the petroleum generation and expulsion (i.e. petroleum phase-type, quality, and amount).

We also plotted the pyrolysis T_{max} data against the hydrogen and production indices (Fig. 11a and b). Using both plots, we obtained information on the source rock maturation levels, sample contamination issues, or samples with low levels of conversion. The plots showed that the main source rocks of the Zallah–Dur Al Abd trough (i.e. the Rachmat and Sirte formations) entered the mature stage (oil window) with a T_{max} ranging from 435 °C to 455 °C, as confirmed by the vitrinite reflectance data (modelling and optical measurements). This suggests that both formations entered the mid-mature stage due to the equivalence of the upper and lower limits to a VRo range of 0.6–0.9%.

4.2.2. Hagfa trough

We selected four wells (C2-16, C1-NC130, A1-94, and D2-10A) to evaluate the source rock maturity levels in the Hagfa trough. The organic matter concentration increases toward the Hagfa trough depocenter, which is located in its northern part, and decreases toward the southwest axis of the trough, structural highs, or carbonate platforms. The Hagfa trough shows multiple source rocks and generative kitchens. The primary source rocks are the shales of marine origin—the Rachmat and Sirte formations. Other source rocks, such as the Etel, Kalash, and Hagfa formations, were also seemingly involved in the process of charging the surrounding platforms with hydrocarbons. Results indicate that the aforementioned source rocks have different levels of thermal maturity, starting from the early maturity levels and reaching over-mature stages with a VRo ranging from 0.5% to 1.7%. The analysis of the deepest well (C1-NC130) located close to the Hagfa trough depocenter indicated that most of the Cretaceous section entered the mid-to late-maturity levels (Fig. 12). The other three selected wells are located farther away from the depocenter as the early petroleum exploration

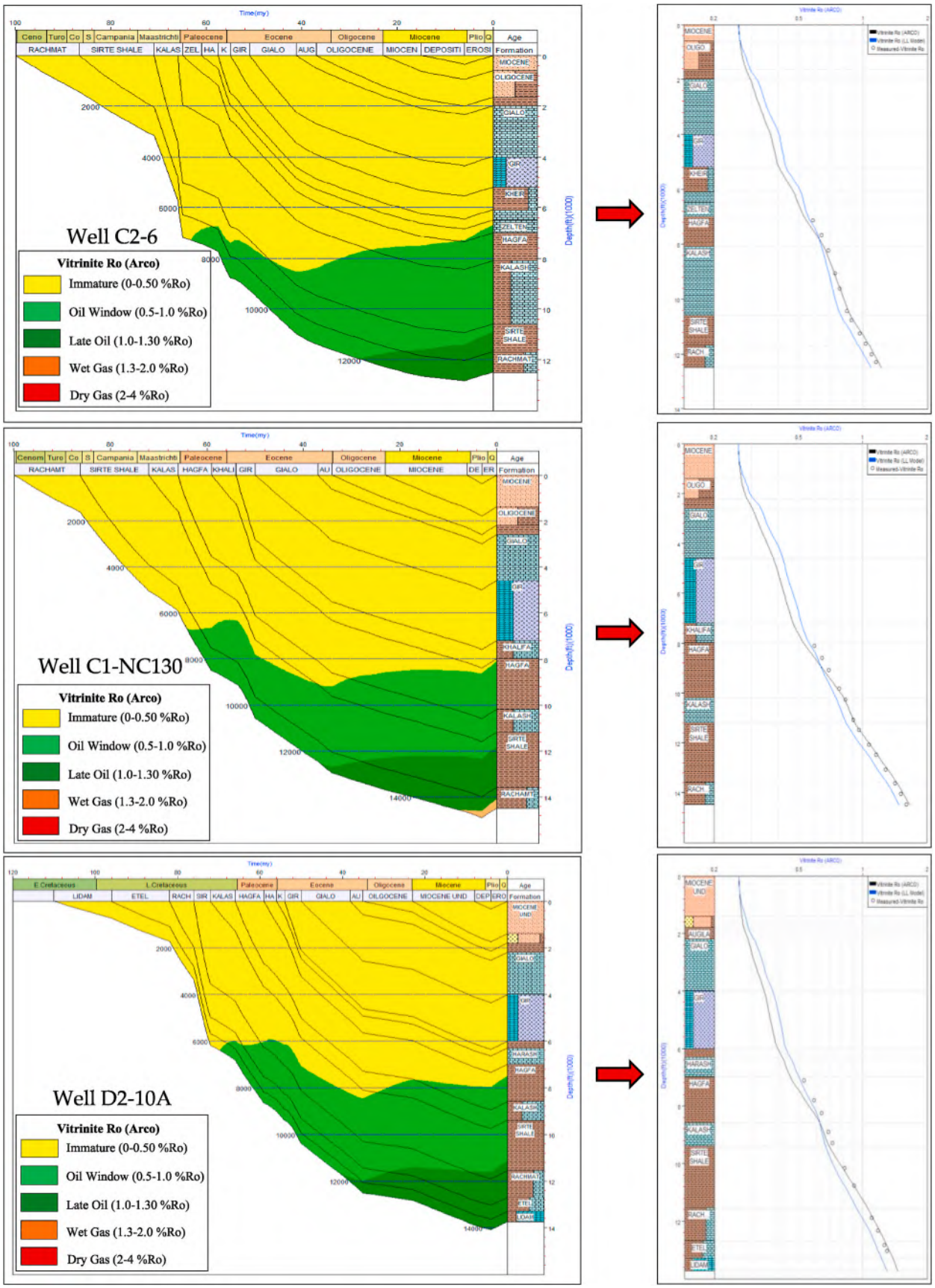

Fig. 12. Burial history models constructed for the Hagfa trough using three selected wells (C2-16, C1-NC130, and D2-10A). The source rock maturity levels differ from well to well according to their location and burial levels. The model data input and output were accomplished using Genesis software.

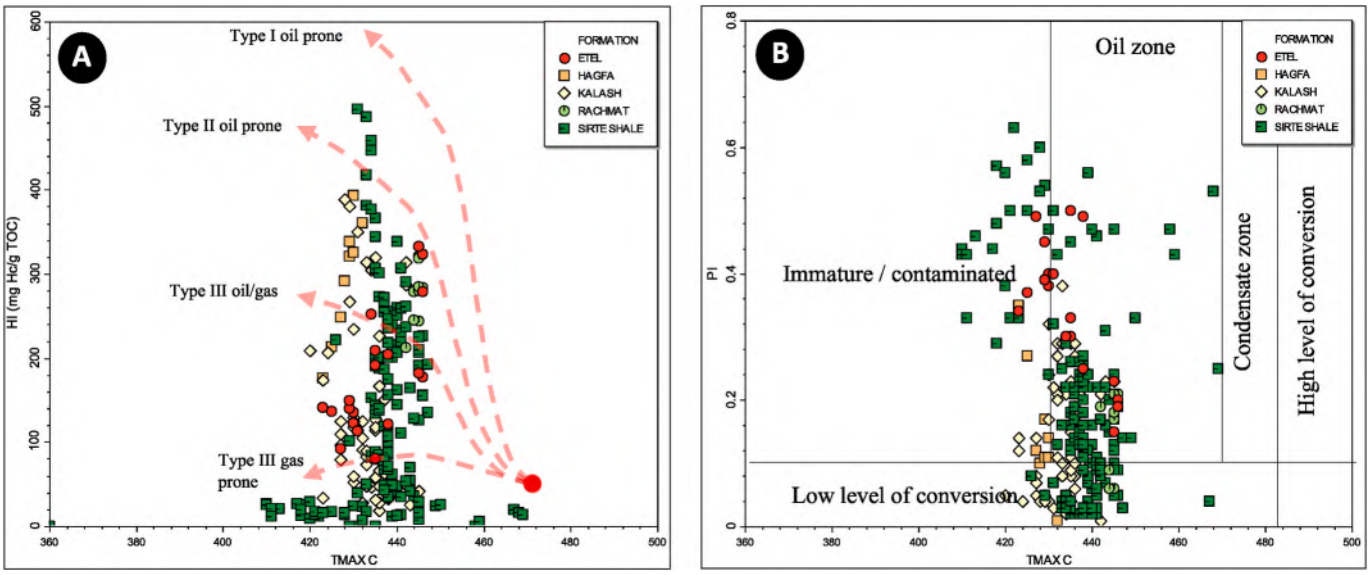

Fig. 13. Thermal maturity levels based on the pyrolysis T_{max} data plotted vs the hydrogen (A) and production indices (B) (wells C2-16, C1-NC130, A1-94, and D2-10A).

efforts in the Sirt Basin were devoted to the exploration on the basin platforms rather than in the troughs, except for a few wells drilled near to the trough depocenter (e.g. C1-NC130). Therefore, we lack enough control data from the depocenter to confirm that the maximum maturity levels occur there. However, we used several extrapolation techniques based on the source rock maturity and the constructed burial history models (maturity as a function of structural trends, see Fig. 25 for more details).

In the Hagfa trough, the Etel Formation shows a VRo averaging near 1.75%, due to deeper burial levels. The Etel Formation was interpreted to be of lacustrine palaeoenvironment origin (Ashour, 1996). Therefore, it shows significant lateral variations in lithology between the salt and shale units. It serves as a good source rock only in the organically rich shale intervals in some troughs of the Sirt Basin, such as the Ajdabiya, Hameimat, and south Hameimat troughs, where higher maturity levels have been attained, and the Etel Formation entered the gas window. The Rachmat Formation's VRo reaches 1.7% (C1-NC130), which is the maximum maturity level detected for this formation, according to the well location and level of burial. The shales of the Sirte Formation suggest that this source rock entered the mid-to late-maturity levels, with an average VRo of 1.35%. The Sirte shales in the Hagfa trough form the basal hydrocarbon generative kitchen prior to the Rachmat shales. Both formations generated and charged the Az Zahra, Al Byda, and western flank of the Zaltan platform with a considerable amount of hydrocarbons. Other source rocks, such as the shales of the Kalash and Hagfa formations, exhibited early to mid-maturity levels, with an average VRo of 0.9%. The T_{max} pyrolysis vs the hydrogen index plot (Fig. 13a) indicates that the data from the Sirte and Rachmat formations fall within the low maturity region ($T_{max} < 430$ °C), indicating a low level of kerogen conversions (additionally indicated by plotting T_{max} pyrolysis vs the production index). This might be related to the presence of low-quality organic matter (Fig. 13b). In contrast, the T_{max} data from the Etel Formation shows a substantially high maturity level attained ($T_{max} > 440$ °C).

4.2.3. *Ajdabiya trough*

According to the previous studies in the Sirt Basin, the Ajdabiya trough is the deepest and most geologically defined. It is bounded by the Nafoora high (platform) in the east, elongated Zaltan platform in the west, and Jahama platform in the northwest (Goudarzi et al., 1980; Ghori, 1996; Abadi et al., 2008). In general, these features were formed in the area due to complex structural processes that occurred during the Sirte Arch collapse and the formation of the tilted grabens and horsts, which caused the two geological features (troughs and grabens) to have an oblique structural orientation stretching from northwest to southeast (Megerisi and Mamgain, 1980). We believe that a proper understanding of the tectonic nature of the Ajdabiya trough and the subsequent development from its initiation until the present day is crucial for understanding the thermal maturation evolution and geographic distribution of the source rocks locally and regionally.

The Ajdabiya trough source rocks are known to be responsible for charging numerous oil, condensate, and gas fields (e.g. the Nafoora and Amal oil fields) in the trough itself and up-dip areas. However, there have been no regional geochemical investigations, except for a few local studies from the eastern and western Sirt Basin based on oil–oil or oil–source correlations to identify the potential source rocks (e.g. groping oils). As shown herein, different troughs in the Sirt Basin are characterised by multiple source rocks that entered the oil and gas windows in different time periods (e.g. the Hagfa trough source rocks) and range in thermal maturity levels from mid-to late-maturity. It is likely that the present-day hydrocarbons were sourced from a mixture of oil families, making it more challenging to reveal the petroleum recharge history.

The calculated geothermal pattern in the Ajdabiya trough averages 1.5 °F/100 ft. In the structural highs, such as the Jahama platform, the values reach 2 °F/100 ft and decrease toward the western part of the trough. Low geothermal gradients in the basin troughs are known to benefit hydrocarbon accumulation. The heat flow determined for the structural highs surrounding the Ajdabiya trough is elevated compared with the Ajdabiya trough with low heat flow records. These observations agree with the predominant lithology encountered in the trough and platforms: low heat conductive rocks are present in the trough compared with the high heat conductive sediments of the surrounding platforms. The basal hydrocarbon generative kitchens in the Ajdabiya trough constitute the Turonian Etel, Coniacian Rachmat, Campanian Sirte, Maastrichtian Kalash, and Danian Hagfa formations deposited in marine to freshwater and saline lacustrine environments. This diversity of depositional environments allowed adequate amounts of rich organic matter with different qualities to accumulate and to participate in charging many discovered oil and gas fields in central of the Sirt Basin.

The Campanian Sirte Formation in the Ajdabiya trough entered the late-to over-maturity levels in the middle Palaeocene at depths of 13,179 ft (4018 m), as indicated by well 4E1-6. This well is considered to

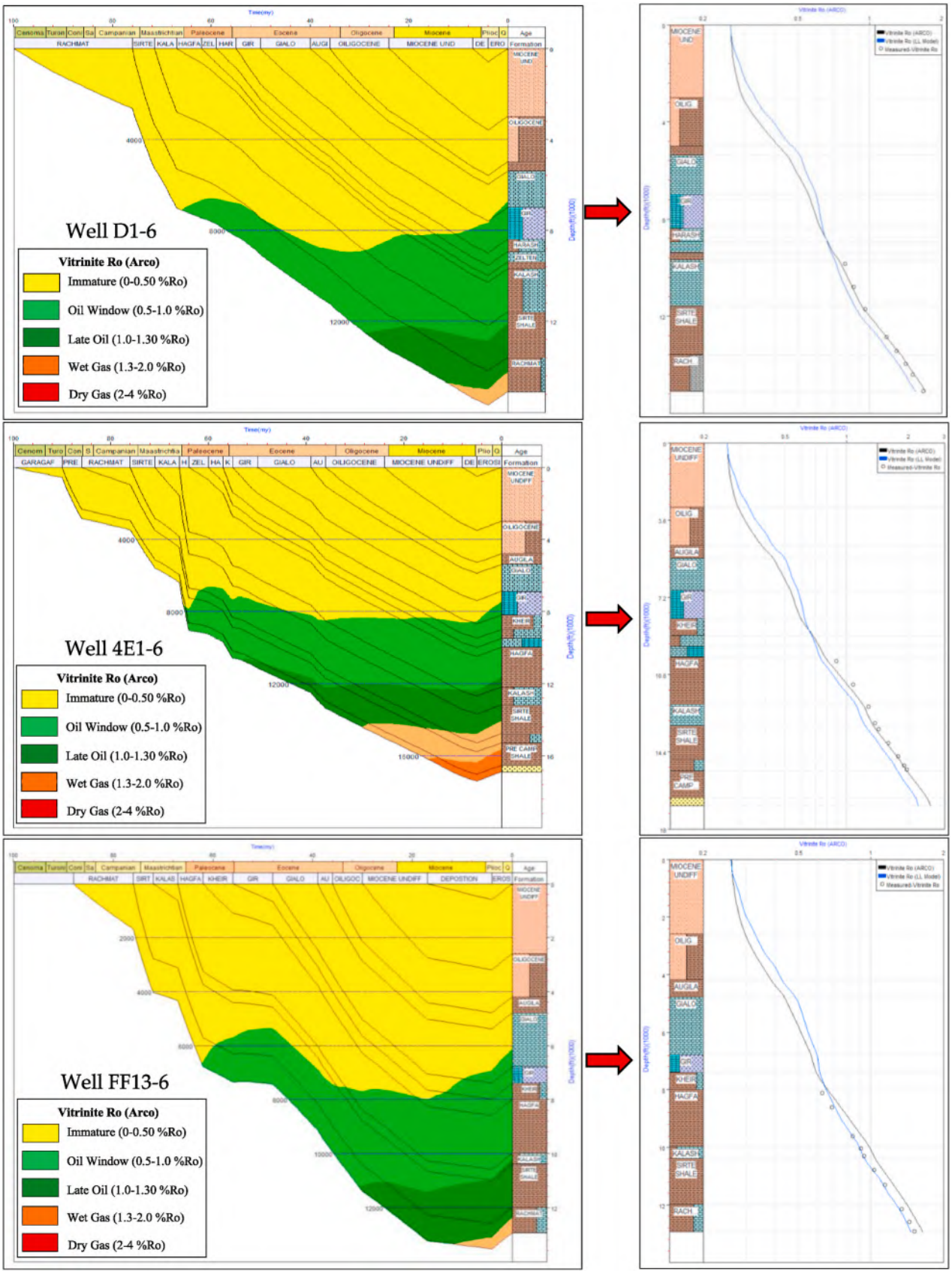

Fig. 14. Burial history models for the Ajdabiya trough obtained from the three typical wells (D1-6, 4E1-6, and FF13-6). The source rock maturity levels differ between the wells according to the burial depth. The model data input and output were accomplished using Genesis software.

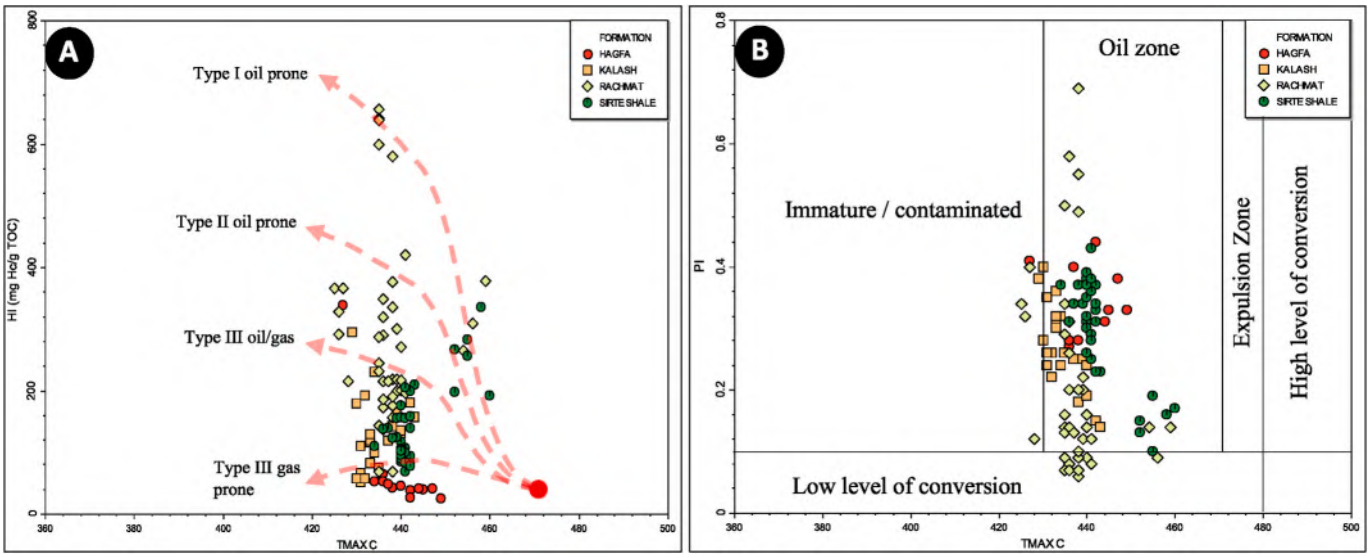

Fig. 15. Maturity levels inferred from the pyrolysis T_{max} data plotted against the hydrogen (A) and production indices (B) using the Ajdabiya trough wells (D1-6, 4E1-6, 3K1-6, and FF13-6).

be the deepest one in the trough to study the thermal maturation levels of the source rocks. It showed that Sirte Formation's VRo reaches 1.6% and has a maximum pyrolysis temperature similar to the Rachmat Formation (460 °C), where an average pyrolysis temperature reached approximately 440 °C (Fig. 14). The Turonian Etel Formation in the Ajdabiya trough was determined to be mature with a VRo of 2%, specifically in the Wadayet trough, where it entered an over-maturity level with type III kerogen. As per the present-day burial models, the Etel Formation entered the gas window and is considered the main recharger of gas in the area due to the high levels of thermal maturity attained at deep burial depths. The gas is currently developed in the Attahaddy, Assumood, N. Arshad, Sahal, and Hateiba gas fields. The 1D burial models related to the Coniacian Rachmat Formation in the Ajdabiya trough showed that this marine source rock entered the over-maturity level with a VRo greater than 1.8% (gas window), as demonstrated by well 4E1-6, at a burial depth range of 14,750–5500 ft. Well 4E1-6 is located in the Jahama platform and is the deepest well in the trough. Therefore, the maturity information obtained from this well is trustworthy. The Kalash Formation has poor to fair source rock qualities in this trough, according to its TOC; however, it entered the over-maturity level with a VRo of 1.5% in the Wadayet area. As per the modelling results, the Hagfa Formation in the Ajdabiya trough entered the mid-maturity level in the deep trough, with a maximum VRo of over 1%.

The plot of the pyrolysis T_{max} data vs the hydrogen index data (Fig. 15a) shows that most of the investigated source rocks fall into the mature category, and a few data points from the upper Hagfa Formation are clustered at the mid-maturity levels with a T_{max} ranging from 430 °C to 470 °C. The production index of the Rachmat Formation is much higher than that of the Sirte Formation, meaning that a higher amount of hydrocarbons was generated by the Rachmat Formation than by the Sirte Formation. Approximately 14 samples from the Rachmat Formation seem to cluster in the zone of low levels of kerogen conversion, whereas most of the samples from the Rachmat and Sirte formations fall in the mid-to late-maturity levels. The Kalash and Hagfa formations are both characterised by low production and reduced hydrogen indices (<200 mg HC/gm TOC) probably because they were affected by the low terrestrial organic matter input (Fig. 15b).

4.2.4. Kotla and Dur Attalha troughs

As reported elsewhere (Hallett, 2002), the past and present exploratory efforts have not been successful, with only a few petroleum discoveries made around the Kotla trough and no discoveries made on the Dur Attalha trough or in the adjacent area of the trough, which is the plausible place for hydrocarbon generation and accumulation. To evaluate the source rock maturity in the Kotla and Dur Attalha troughs, we selected four wells, two of which are situated in the Kotla trough, and the other two in the Dur Attalha trough. In the Kotla trough, the maturity levels in both wells (G1-47 and B1-93) were not higher than 1.5%, as suggested by the VRo data. Well G1-47 showed a good correlation between the Arco model and VRo in its lower section, with a minor value separation in the upper section. Other wells also fitted well (Fig. 16).

As indicated by the deepest well (G1-47), the Coniacian Rachmat Formation, with its dominant type II/III kerogen and a HI of over 400 mg HC/gm TOC, entered the mid-maturity level with a VRo of less than 1% in the early Palaeocene (~68 Ma). The results obtained from the calibrated burial history models revealed that this level of maturity continued until the late Miocene (~5 Ma), with a burial depth of approximately 7500 ft (2286.5 m). The source rock maturity results acquired from well G1-47, which is situated near the trough depocenter, were regarded as indicative and sufficient.

The burial history models constructed for this area (wells, B1-93, G1-47, and H1-72) suggested that the burial continued until the late Miocene, and a substantial uplift occurred immediately after that. The Sirte Formation results demonstrated that type II/III (dominantly II) kerogen prevailed with a HI of less than 600, indicating that the Sirte Formation shales were characterised by organic matter input from multiple sources with a TOC value greater than 1%. The Sirte Formation is responsible for the main petroleum accumulations on the Al Bayda platform and Gattar Ridge. However, the Sirte shales at a depth interval of 8300–10,000 ft (457–3048 m) showed mid-maturity levels with a VRo ranging 0.6–1%, similar to the Rachmat Formation in well G1-47. The Kalash and Hagfa formations in the Kotla trough have less significant potential for hydrocarbon generation than the Etel Formation. The Kalash Formation presented a mid-maturity level, whereas the shales of the Hagfa Formation acquired only an early maturity level, with a VRo ranging between 0.3% and 0.5%, based on the results from well G1-47. Both the Kalash and Hagfa formations demonstrated early maturity levels, based on the VRo results from B1-93; this well is shallower than G1-47.

The Dur Attalha trough presented source rock maturity levels higher than Kotla trough, with high maturity levels at the deeper levels of the trough (depocenter), which is in fact quite deeper than the Kotla trough. Due to the general lack of control data (well information), we were able to use only two wells for maturity modelling. Well H1-72 was used to

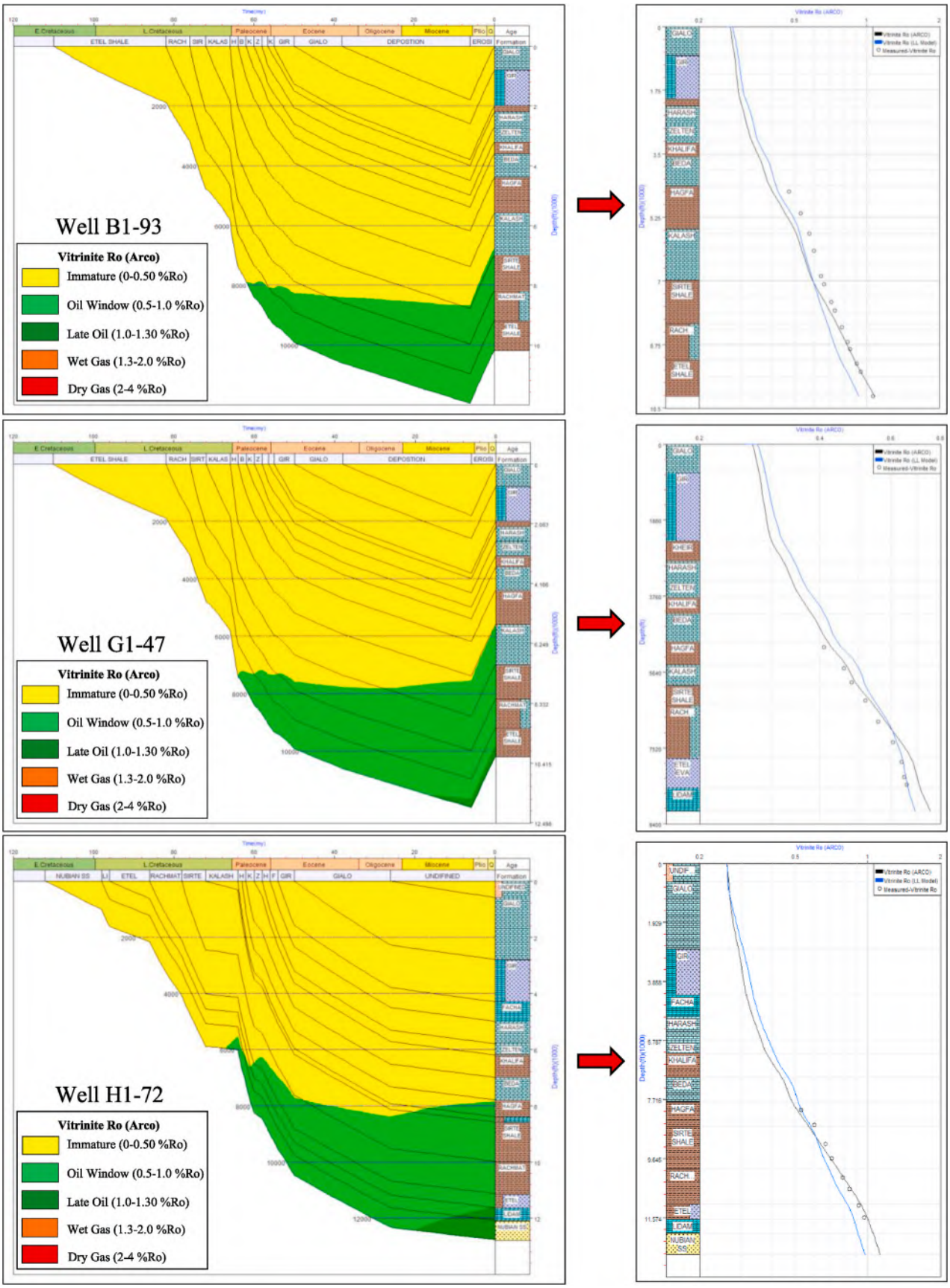

Fig. 16. Burial history models for the Kotla and Dur Attalha troughs based on the three selected wells (G1-47, B1-93, and H1-72). The maturity levels differ between the wells depending on their burial depths. The model data input and output were accomplished using Genesis software.

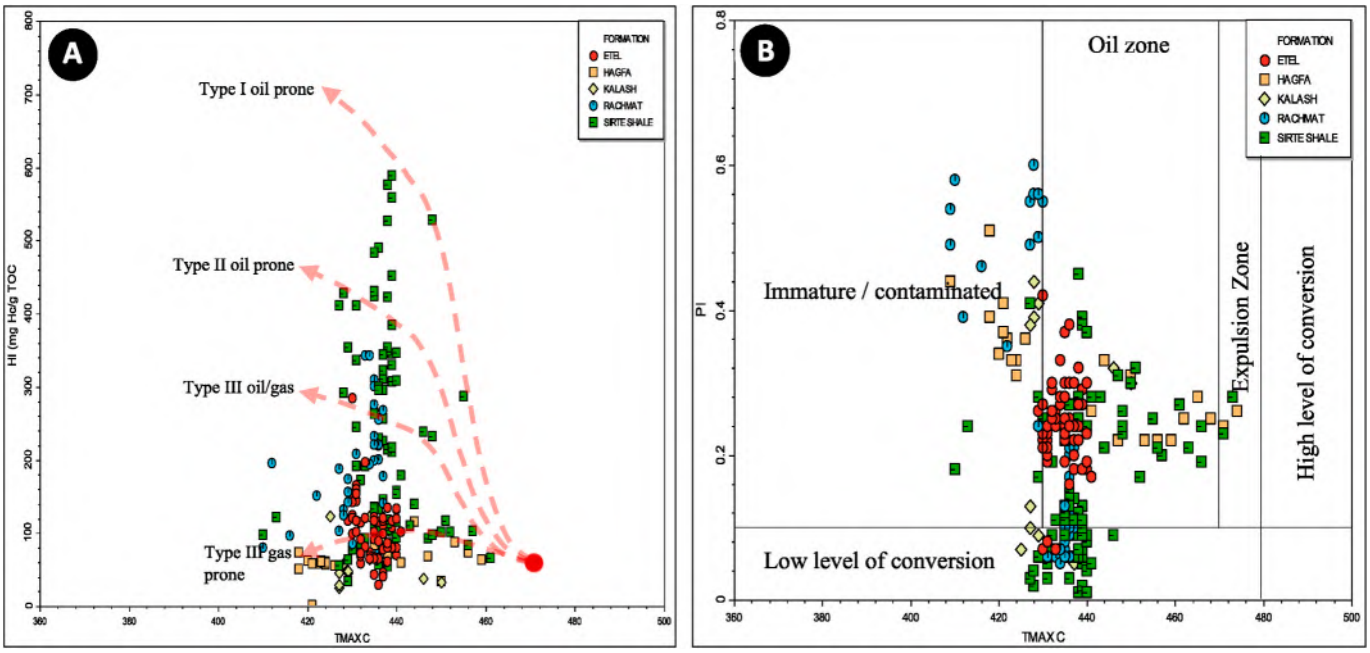

Fig. 17. Plots of the pyrolysis T_{max} data vs the hydrogen (A) and production indices (B). The data were obtained from the Kotla and Dur Attalha trough wells (G1-47, B1-93, H1-72, and E1-72).

investigate maturity levels. The constructed 1D burial history models showed that there was no strata uplift at the end of the Miocene in contrast to the Kotla trough. Therefore, the source rocks of the Dur Attalha trough experienced continuous burial until the present-day time. As a result, the Etel, Rachmat, Sirte, and Hagfa formations entered the mid-maturity level, which allowed the organic matter to convert to hydrocarbons, generate and probably expel sufficient amounts of petroleum.

The maturity levels obtained from the pyrolysis T_{max} data were similar to the VRo analysis results, indicating that the Cretaceous source rocks reached the mid-to late-maturity levels (430–445 °C). Plotting the pyrolysis T_{max} data vs the hydrogen index (Fig. 17a) allowed us to quickly assess the source rock kerogen type and degree of maturity. Most of the shales in the Upper Cretaceous Rachmat and Sirte formations contain type I/II kerogen (oil- and gas-prone source rocks), whereas the shales of the late Palaeocene Hagfa and Early Cretaceous Etel formations are characterised by the late-maturity levels with dominant type III kerogen (gas-prone source rocks). The production index plotted against the pyrolysis T_{max} data (Fig. 17b) indicated that most of the data points clustered in the oil zone, whereas over 20 samples from the Sirt, Rachmat, and Etel formations clustered in the zone with low conversion levels. The plot also suggested that the data with a T_{max} of less than 430 °C might be affected by contamination or those samples were initially immature.

4.2.5. *Eastern Sirt Basin troughs*

The eastern part of the Sirt Basin is a prolific hydrocarbon province with several supergiant oil fields, such as the Amal, Augila-Nafoora, and Sarir. Petroleum is produced from the Precambrian to Oligocene reservoirs characterised by low nitrogen, oxygen, and sulfur (NOS) content and often highly waxy oils (Ahlbrandt, 2001; Alghanduri et al., 2010; Hallett, 2016). The kerogen type varies in the eastern Sirt Basin troughs, with types I/II/III kerogen being the predominant ones. All of them are related to different organofacies (organic facies) and likely originated from different organic precursors. It is important to evaluate the source rock thermal maturity degree using various analytical and modelling techniques, especially in this rich and active petroleum province of the Sirt Basin, to estimate the undiscovered petroleum resources. Our unpublished regional geochemical correlations indicate that the source rocks in the eastern Sirt Basin strongly vary in their TOC, both laterally and vertically. Such a variation might be related to the organic matter type, its amount, original palaeoenvironments of deposition (e.g. marine, lacustrine), and preservation conditions in the host troughs (e.g. stable anoxic conditions).

The source rock maturity assessment and geochemical screening in the eastern Sirt Basin were accomplished using nine selected typical wells (NN1-82, II-65, OO1-65, D1-NC98, R1-65, D1-51, A2-96, and 5Q1-59). The Mid Nubian, Etel, Rachmat, Sirte, and Kalash formations are the local source rocks in this area and show variable maturity levels in different locations. These five classes of source rocks principally charge petroleum in this part of the basin. However, Burwood et al. (2003) analysed the petroleum system of the eastern Sirt Basin and emphasised that other less important source rocks also participated in the present-day hydrocarbon accumulations.

The Lower Cretaceous source rocks in the eastern Sirt Basin include the Mid Nubian and Etel formations. Based on the constructed burial history models, their thermal maturity ranges between the mid- and late-mature stages (0.6–1.35% VRo). Well D1-NC98 is located in the Hameimat trough and was used to demonstrate that the Lower Cretaceous source rocks entered the late-mature stage (Fig. 18), with the Hameimat trough being the deepest among the other eastern Sirt Basin troughs. The burial levels of the Lower Cretaceous source rocks in the Hameimat (main) and the southern Hameimat troughs reached 14,000 ft (4258 m), up to the bottom of the Mid Nubian Formation (Fig. 19). The Lower Cretaceous source rocks are mature in the Feregh (5Q-59), Sarir (OO1-65), and Maragh troughs (A2-92). These troughs have accumulated over 20 oil fields, including the giant oil fields, such as the Amal, Nafoora, and Sarir.

The Upper Cretaceous source rocks, including the Rachmat, Sirte, and Kalash formations, became mature at different geological times. For instance, the analysis of well D1-NC198 suggested that the Rachmat Formation achieved the mid-maturity level in the early Eocene (55 Ma) at a burial depth of approximately 8400 ft (2561 m), whereas the Sirte Formation entered this maturity window much later in the mid of Eocene (~40 Ma). However, the Upper Cretaceous source rocks entered the oil window at different geological times as a function of the thermal

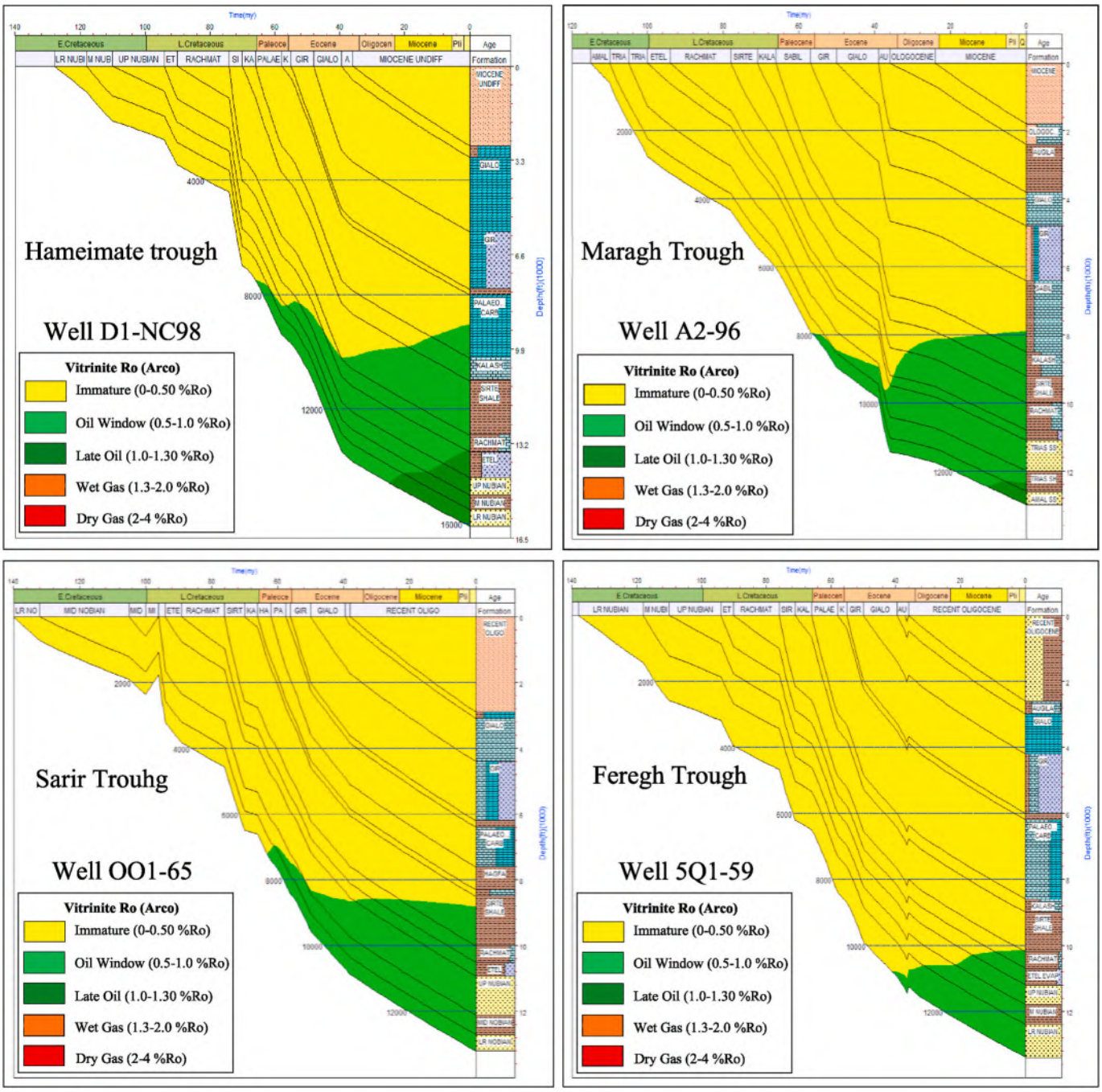

Fig. 18. Calibrated burial history models of the four selected typical wells. The Arco model was used to identify the maturity levels in each of the eastern Sirt Basin troughs, including the Hameimate, Maragh, Sarir, and Feregh troughs.

maturity and burial depth, providing us with a good understanding of the timing of petroleum generation, petroleum expulsion, trap formation, and charge history. The details of the petroleum generation, expulsion, and charge mechanisms in the eastern Sirt Basin have not been defined yet, making many petroleum geologists believe that the late Palaeocene source rocks might have accumulated the reservoirs with petroleum in this part of the basin. However, the results of the 1D burial models constructed herein did not support this idea and showed that the Palaeocene source rocks are in the early mature stage, even though their organic content in some parts of the basin exceeds 1% TOC. However, with such a low level of maturity, the kerogen would not have transformed into oil and produced commercial petroleum accumulations. According to our data, the basal source rocks in the basin are limited to the shales of the Triassic and Cretaceous ages.

Thermal maturity levels in the prolific parts of the eastern Sirt Basin ranged from the early maturity (0.5% VRo) to late-maturity (1.35% VRo). The pyrolysis T_{max} data plotted vs the hydrogen index data (Fig. 20a) from the five primary source rocks (Mid Nubian, Etel, Rachmat, Sirte, and Kalash) indicated the variations in the maturation levels. We considered the source rock immature when its T_{max} was less than 430 °C; the early mature stage was attributed when T_{max} ranged between 430 °C and 435 °C; the strata became mature when T_{max} ranged between 435 °C and 455 °C; the late-mature stage was ascribed when T_{max} ranged from 455 °C to 470 °C; and, finally, the strata was overmature when T_{max} exceeded 470 °C. The plotted values ranged from 420 °C to 457 °C, representing the immature to late mature source rocks.

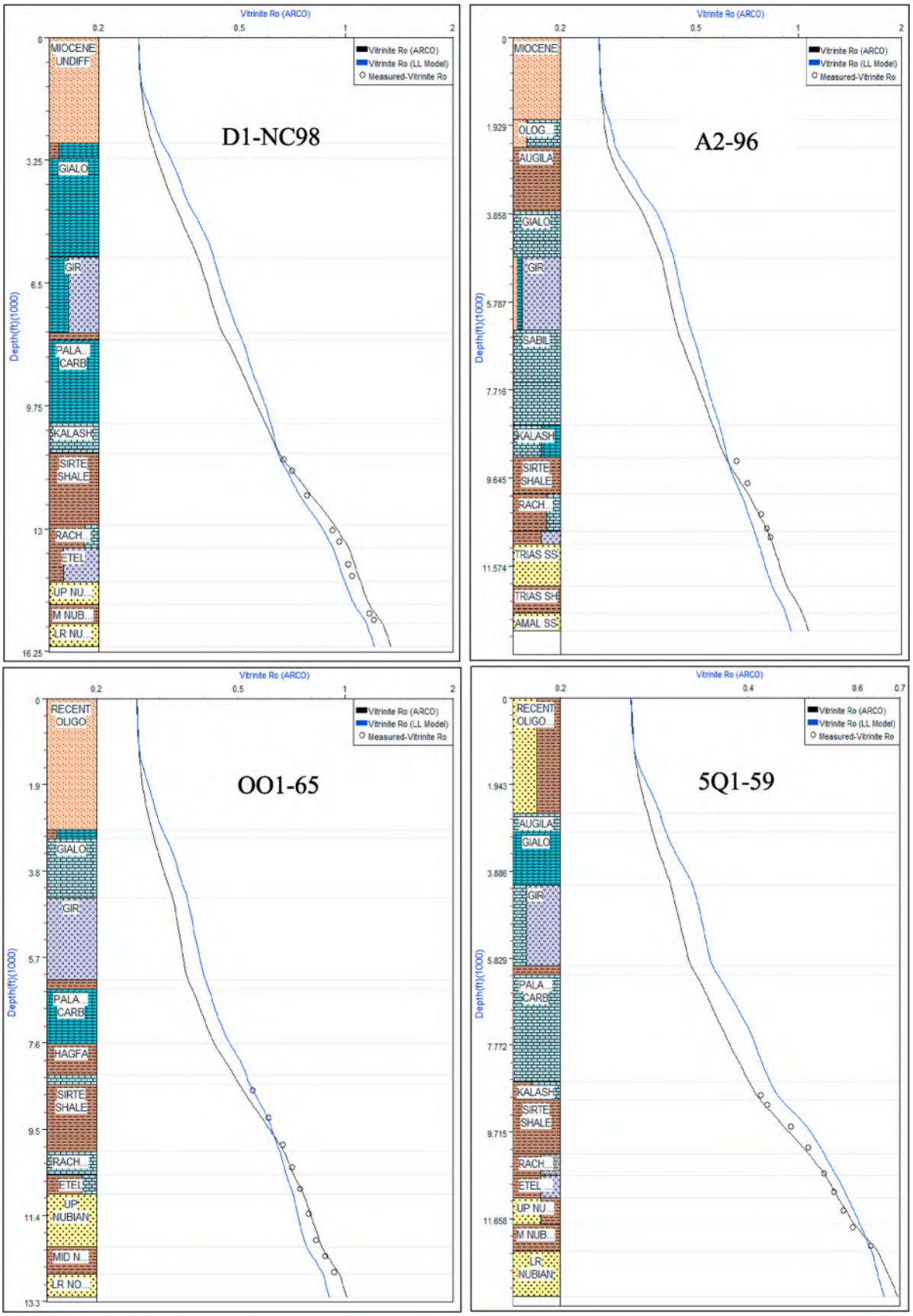

Fig. 19. Calibrated 1D maturity models in some typically selected wells in the eastern of Sirt Basin troughs were the two simulated %VRo have been obtained by using the Arco (black Curve) and LLNL model (Blue Curve) plotted versus the measured %VRo data (model input and output were done by using Genesis software).

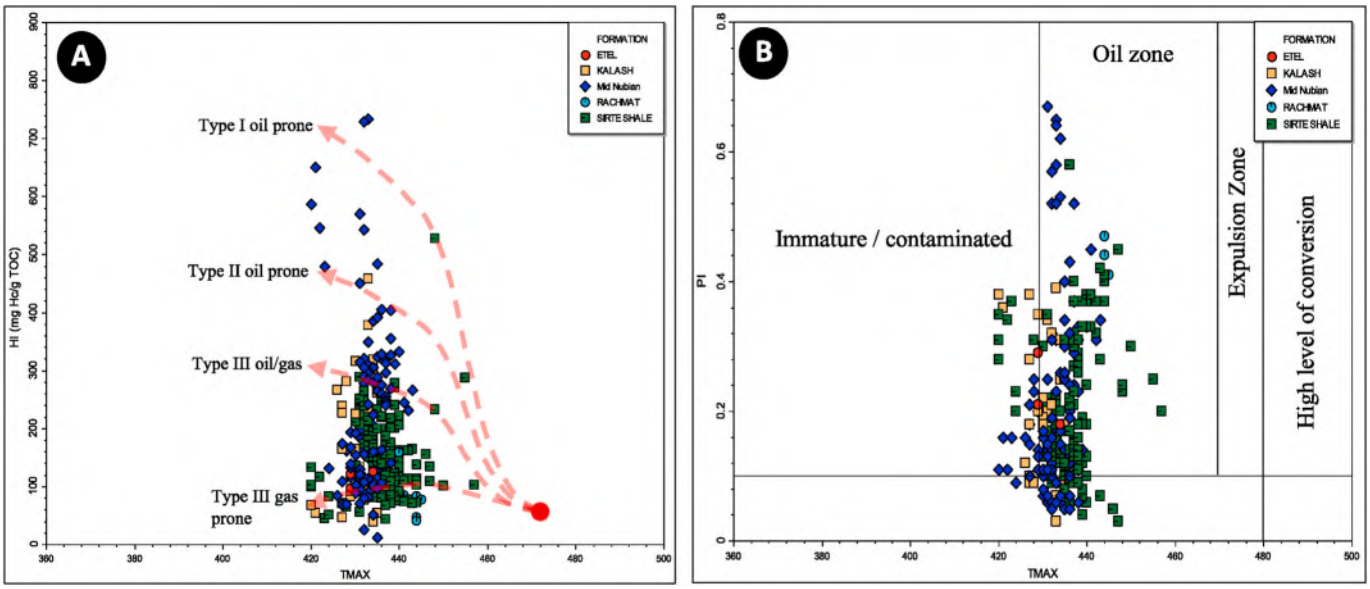

Fig. 20. Thermal maturity inferred from plotting the pyrolysis Tmax data vs the hydrogen (A) and production indices (B) (wells LL1-82, NN1-82, II-65, II-65, L1-65, OO-65, D1-NC98, R1-65, D1-51, A2-96, and 5Q1-59).

These results were consistent with those obtained from measured VRo and model-simulated maturation. The plot between the pyrolysis T_{max} data against the production index (Fig. 20b) revealed that approximately 70% of the samples from those five main source rocks in the eastern Sirt Basin belong to the oil zone, with some samples being contaminated and in a low level of kerogen conversion.

5. Generalised maturity models (1D and 2D)

The geographical distribution and volumetric analysis of the source rocks in the Sirt Basin have not been properly addressed since the commencement of petroleum exploration and production, except for a few local studies. Besides revealing the source rock distribution, it is essential to construct regional source rock maturity maps in the Sirt Basin. The regional maturity maps for each source rock in the Sirt Basin were created using the top surface of each source rock. The construction of each horizon using formation tops was done initially using the correlation gridding method by creating the tops from dense well information data, and secondly, using the correlation gridding techniques to obtain the rest of the formation tops throughout the basin. The results of the constructed maturity maps using the LLNL model were calibrated and checked for their validity against the widely used direct thermal maturity indicators (e.g. vitrinite reflectance and pyrolysis T_{max} data). The Upper Cretaceous and late Palaeocene sections in the Sirt Basin showed similar VRo values ranging from 0.3% to 2% (Fig. 21, Fig. 22, and Fig. 23).

The generalised 1D burial history models were constructed based on 25 typical selected wells from different locations of the Sirt Basin using the Arco and LLNL modelling approaches. Both models were constructed and calibrated in conjunction with the measured VRo data (Fig. 24). We decided to generalise the 1D thermal maturity trends in the Sirt Basin to predict thermal maturity for all minor active source rocks in the basin as the maturity converted to be a function of the burial depth. The application of maturity trends to the Harrash, Triassic shale and Khalifa formations in the Sirt Basin can provide the petroleum geologists with a better idea on their degree of thermal maturation, even when the samples or data are not available. Although some previous studies indicated that they might have some petroleum potential, no detailed descriptions of their attained maturation level, thickness, or geological distribution in the Sirt Basin have been published. Based on the results presented herein, the Sirt Basin prospectivity does not exclusively depend on the Sirte and Rachmat Formations as the principal source rocks, but also on the other source rocks, such as the Triassic shale in the Maragh trough. The Triassic shale has been distinguished by its substantial areal distribution, thickness, high organic-matter quality, and sufficient thermal maturity to generate commercial quantities of petroleum. We regard the Sirt Basin as promising for the future petroleum exploration of both conventional and unconventional reservoirs. This study provides only preliminary information on the maturity levels of each Sirt Basin source rock. These data can be used for the initial evaluation of the unconventional resources; for example, shale gas plays in the Sirt Basin have never been subjected to detailed studies regarding their future economic importance due to lack of good understanding to the source rock distribution and their geochemical characteristics.

The overall maturity of the Sirt Basin source rocks was determined to be between 0.3% and 2% VRo, with the highest maturity levels (late-to over-maturity) reached in the deepest troughs, such as the Hagfa and Ajdabyia troughs. We consider that the best way to understand the systematic variations and trends in the source rock thermal maturity at a regional scale is to superimpose the maturity maps with the source rock formation tops (structural maps), thereby providing a clear picture of the systematic increase or decrease in thermal maturity toward the basin troughs or platforms (e.g. Fig. 25). We also applied the VRo data derived from the Sirt Basin source rocks to the constructed maturation model. It allowed us to provide more clarity in summarising the maturity levels for each source rock in the basin.

6. Summary and conclusions

1) Due to the variation and complexity in the source rock maturation levels in the Sirt Basin, petroleum geologists need a better understanding of the burial histories (geohistories), tectonic evolution, subsidence, sedimentation processes, geothermal gradient, heat flow patterns, and heat conductivity. All these parameters control the degree of the source rock maturity in the Sirt Basin.
2) The geothermal gradient in the Sirt Basin was 1.58 °F/100 ft on average and demonstrated variable patterns in different locations throughout the basin. Lower geothermal gradients were obtained in the Sirt basin troughs, whereas higher geothermal gradients seem to be a function of the lithology and porosity of the rocks deposited on the basin structural highs (e.g. carbonates). The Sirt Basin heat flow was determined to be uniform and averaged 72 m.W.m^{-2}. The heat

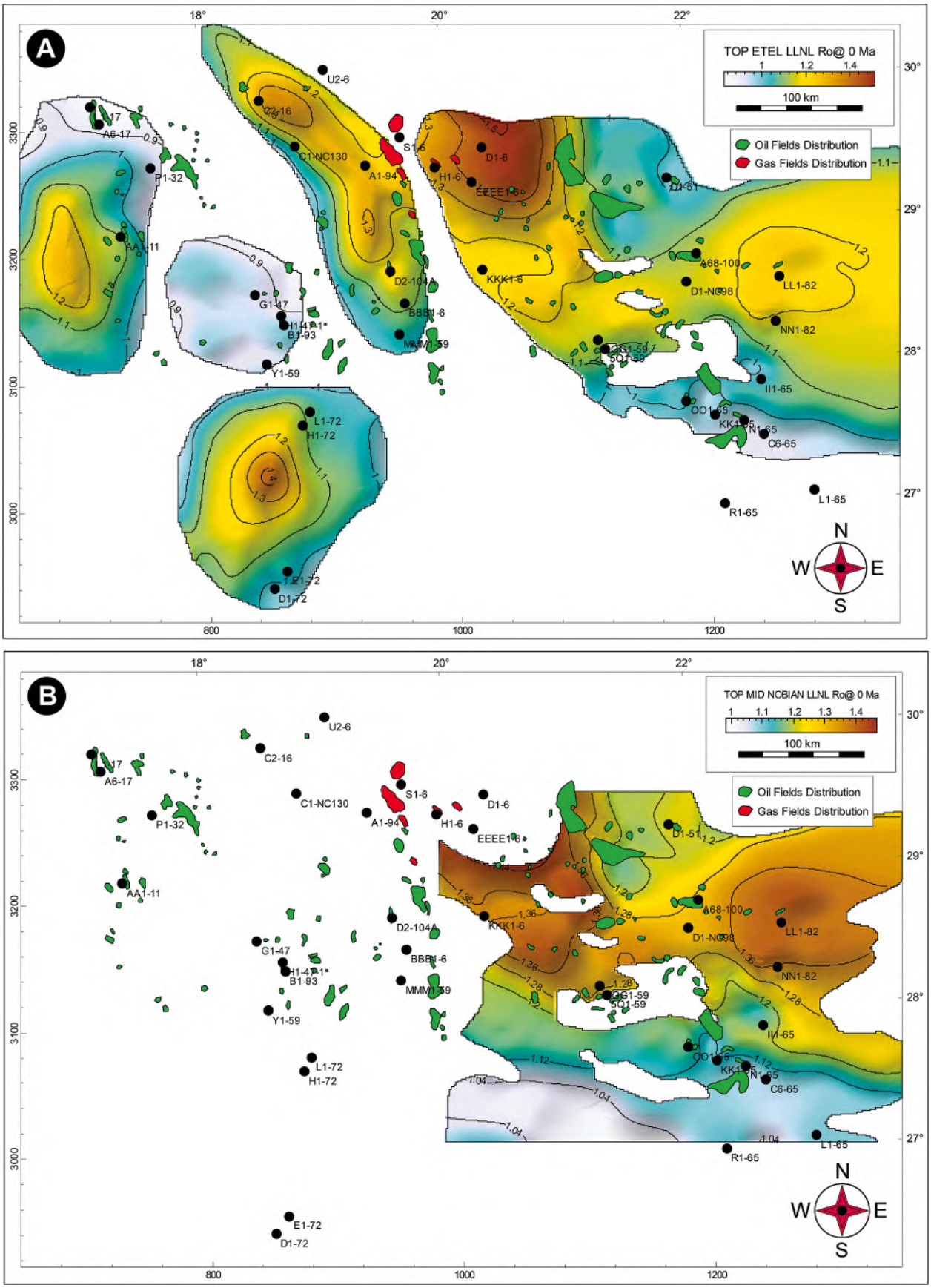

Fig. 21. VRo maps were simulated using the LLNL model calibrated against the 1D burial history models (black dots) for further maturity corrections for the Etel (A) and Mid Nubian (B) formations.

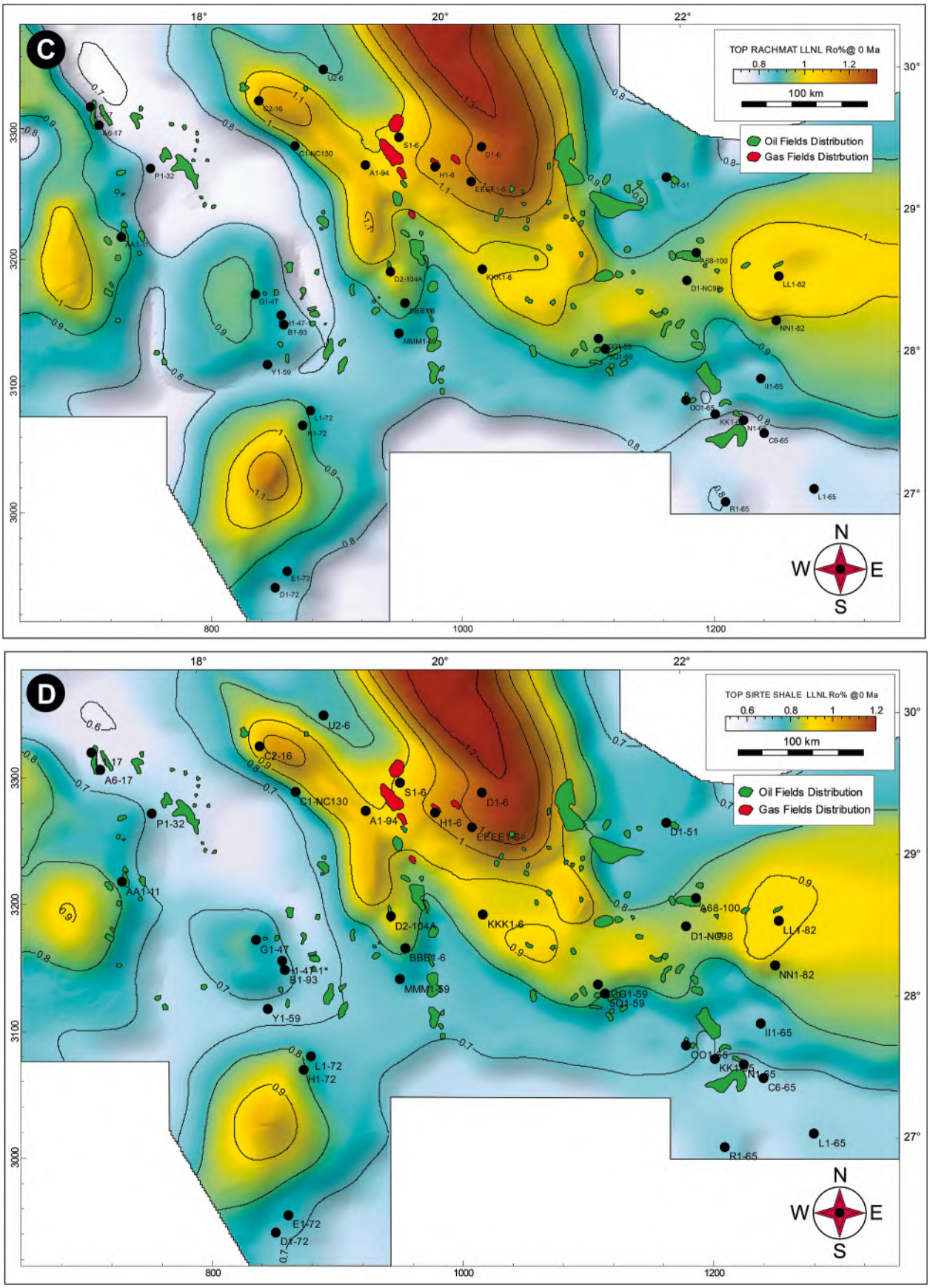

Fig. 22. VRo maps simulated using the LLNL model calibrated against the 1D burial history models (black dots) for further maturity corrections for the Rachmat (C) and Sirte (D) formations.

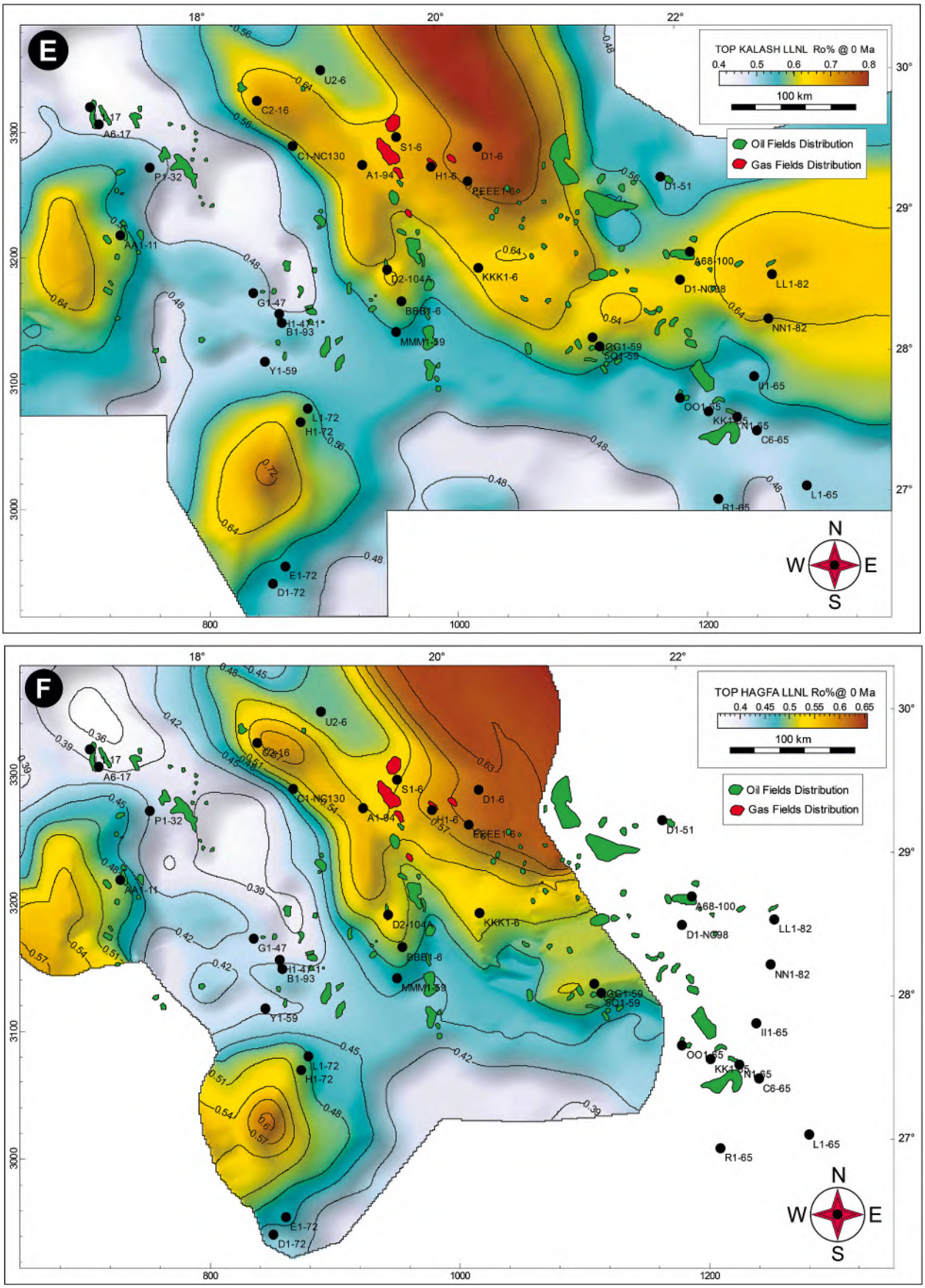

Fig. 23. VRo maps simulated using the LLNL model calibrated against the 1D burial history models (black dots) for the Kalash (E) and Hagfa (F) formations.

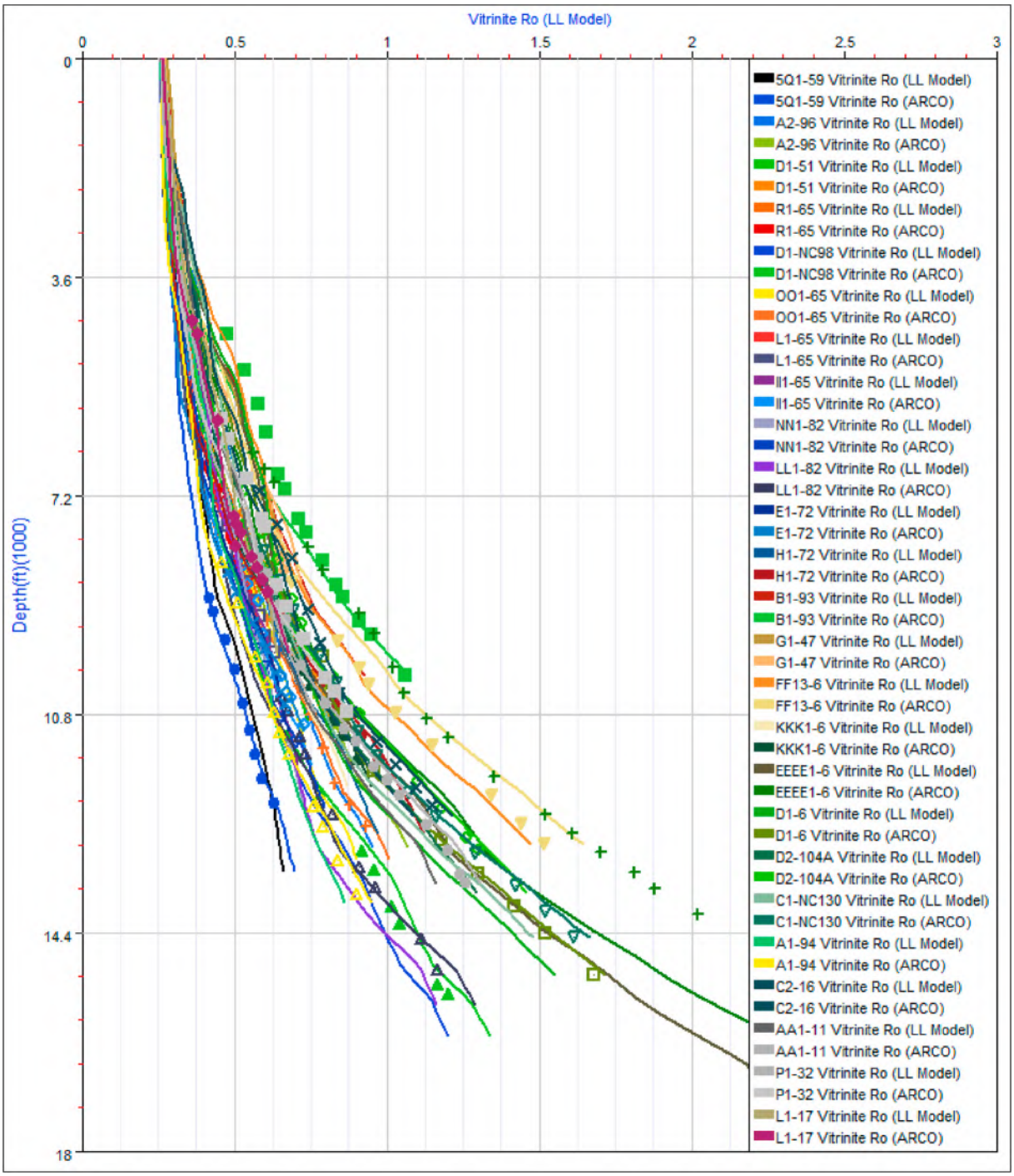

Fig. 24. Generalised 1-D calibrated maturity model of the Sirt Basin based on 25 typical selected wells. The calibration has been utilised using measured %VRo were the model is generated using two modelling techniques (Arco and LLNL with the help of Genesis Software).

flow modelled in the basin troughs was lower than that on the structural highs, similar to the normal geothermal gradient distribution in failed rift basins.

3) The maturity of the six studied source rocks in the Sirt Basin was based on the measured and simulated VRo data. The pyrolysis T_{max} data in some of the selected wells located in the basin troughs indicated that the maximum maturation level was obtained based on the data acquired and simulation results from these wells.
4) In the western Sirt Basin, in the Zallah–Dur Al Abd troughs, we diagnosed three primary maturation levels: early maturity, mid-maturity, and late-maturity. Both the Rachmat and Etel source rocks reached the late-maturity level. The Sirte, Kalash, and Hagfa formations only reached the mid-maturity level, as demonstrated by well AA1-11.
5) Four wells were selected to identify four levels of maturity in the Hagfa trough: early maturity, mid-maturity, late-maturity, and over-maturity. Well C1-NC130 showed that the Rachmat Formation was over-mature, the shales of the Sirte Formation entered the late-maturity level, and the Kalash and Hagfa formations are currently mid-mature. The mid-maturity level in this trough was initiated from the early Palaeocene, whereas the late-maturity level was reached in the middle Eocene and continues to the present day.

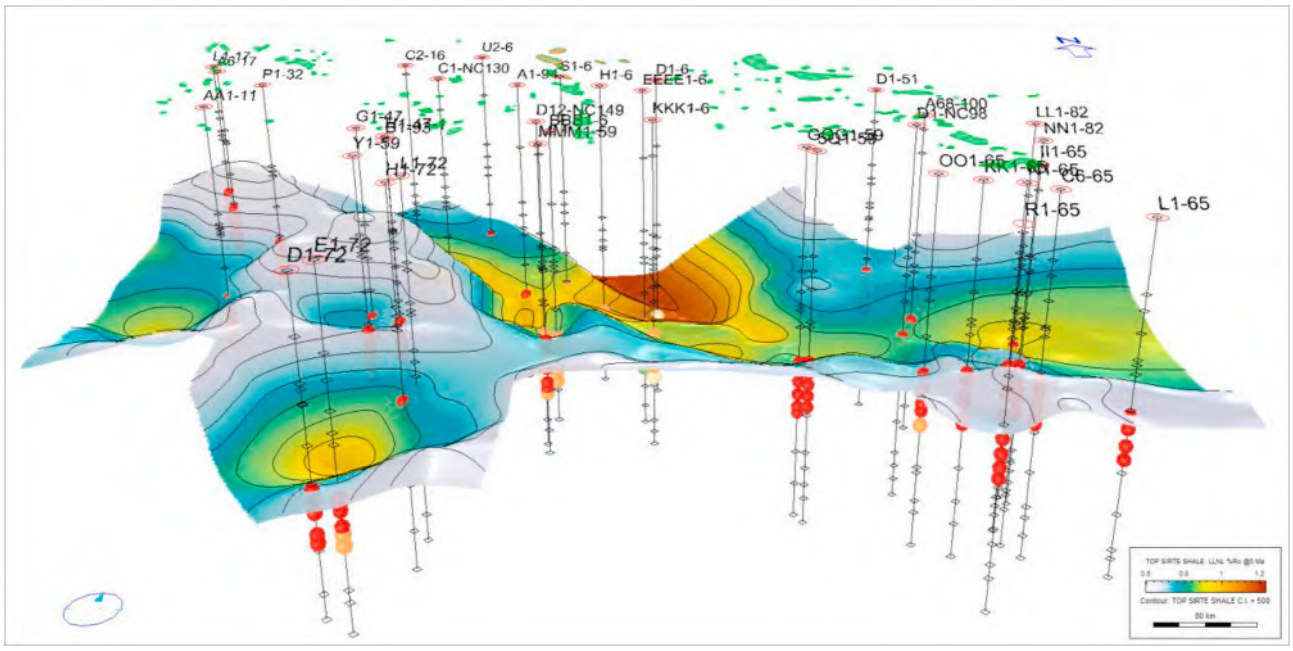

Fig. 25. Calibrated thermal maturity distribution model of the Sirte Formation based on the LLNL model. The modelling results were used to define the maturity trends throughout the Sirt Basin. The Genesis 1D burial history model was utilised to integrate the Trinity (T3) data for further corrections (e.g., formation tops, thickness, thermal gradient, heat flow, and thermal maturity).

6) The Ajdabiya trough is the deepest trough of the Sirt Basin and is located in its north-central part. The sedimentary fill of the Ajdabiya trough reaches 8000 m. Based on the data from well 4E1-6, four primary maturity levels were identified: early maturity, mid-maturity, late-maturity, and over-maturity. The Rachmat and Sirte formations are buried at depths below 12,000 ft (3658 m) and entered the late-to over-maturity levels. The upper part of the Sirte Formation represents the late-maturity level with a VRo ranging 1–1.35%. The Kalash and Hagfa formations both attained mid-maturity.
7) The Kotla and Dur Attalha troughs are characterised by the mid-mature source rocks. However, the shales with the late-maturity levels were found in the trough depocenter, as indicated by the developed maturity maps.
8) The maturity in the eastern Sirt Basin was assessed in four main troughs (i.e. the Maragh, Hameimat, Sarir, and Faregh troughs) which significantly varied. Using nine selected wells in these troughs, three primary levels of maturity were recognised: early maturity, mid-maturity, and late-maturity. The burial history trends (1D) from the constructed models in these four mentioned troughs showed that the troughs were still subjected to continuous burial to the present day.
9) We conclude that the eastern Sirt Basin is dominated by four source rocks, based on their quality and thermal maturities (i.e. the Mid Nubian, Etel, Rachmat, and Sirte formations). We recommend carrying our more detailed work in the Sirt Basin, such as simulating kerogen transformation ratios and constructing 1D and 2D models for each source rock, migration path models, kerogen kinetics, petroleum generation, and expulsion history models to quantify the amount of petroleum expelled from these source rocks.

Declaration of competing interest

The authors declare that they have no known competing financial interests or personal relationships that could have appeared to influence the work reported in this paper.

Acknowledgements

The authors would like to thank the Libyan National Oil Corporation (LNOC) for their help in providing some of the data used in this study. Special Abrams from the Imperial College, London, for his suggestions and critical comments on the earlier version of this manuscript. We are thankful to Dr. Zhiyong He for providing the petroleum system analysis tools for this study (Zetaware, Inc). Special thanks are also extended to our colleagues for their support and encouragement during this study. We thank Yousef Mousa from the Arabian Gulf Oil Company (AGOC) and Tariq Mohammed from the Waha Oil Company (WOC) for their unlimited support. Finally, we thank the editors Dr. Damian Delvaux, William Bosworth, and an anonymous reviewer for their efforts to improve this manuscript and their constructive comments.

Appendix A. Supplementary data

Supplementary data to this article can be found online at https://doi.org/10.1016/j.jafrearsci.2021.104114.

References

Abadi, A.M., 2002. Tectonics of the Sirt Basin. Inferences from Tectonic Subsidence Analysis, Stress Inversion and Gravity Modeling. PhD thesis. Vrije University, Amsterdam, the Netherlands, p. 187.

Abadi, A.M., Wees, J.D., van, M.P., Dijk, V., Cloetingh, S.A.P.L., 2008. Tectonics and subsidence evolution of the Sirt basin, Libya. AAPG Bull. 8, 993–1027. https://doi.org/10.1306/03310806070.

Abdunaser, K.M., McCaffrey, K.J.W., 2014. Rift architecture and evolution: the Sirt Basin, Libya: the influence of basement fabrics and oblique tectonics. J. Afr. Earth Sci. 100, 203–226. https://doi.org/10.1016/j.jafrearsci.2014.06.020.

Abdunaser, K.M., Mccaffrey, K.J.W., 2015. Tectonic history and structural development of the Zallah–Dur al Abd sub-basin , western Sirt basin , Libya. J. Struct. Geol. 73, 33–48. https://doi.org/10.1016/j.jsg.2015.02.006.

Aboglila, S., Elkhalgi, M., 2013. Organic geochemical evaluation of cretaceous potential source rocks, east Sirte Basin, Libya. Int. J. Geosci. 4, 700–710. https://doi.org/10.4236/ijg.2013.44065.

Aboglila, S., Grice, K., Trinajstic, K., Dawson, D., Williford, K.H., 2010. Organic geochemistry use of biomarker distributions and compound specific isotopes of carbon and hydrogen to delineate hydrocarbon characteristics in the East Sirte Basin (Libya). Org. Geochem. 41, 1249–1258. https://doi.org/10.1016/j.orggeochem.2010.05.011.

Ahlbrandt, T.S., 2001. The sirte basin province of Libya–Sirte-Zelten total petroleum system. In: U.S. Geological Survey Bulletin 2202-F, p. 29.
Alghanduri, L.M., Elgarni, M.M., Daridon, J.L., Coutinho, J.A.P., 2010. Characterization of libyan waxy crude oils. Energy Fuels 24, 3101–3107. https://doi.org/10.1021/ef1001937.
Allen, P.A., Allen, J.R., 2013. Basin Analysis: Principles and Application to Petroleum Play Assessment, vol. 3. Wiley-Blackwell, London, pp. 343–367.
Ambrose, G., 2000. The geology and hydrocarbon habitat of the Sarir sandstone, S.E Sirt basin, Libya. J. Petrol. Geol. 23, 165–191. https://doi.org/10.1111/j.1747-5457.2000.tb00489.x.
Ameed, K., Ghori, R., Mohammed, A., Rajab, 1996. The application of petroleum generation modelling to the eastern Sirt Basin. In: Salem, M.J., El-Hawat, A.S., Sbeta, A.M. (Eds.), The Geology of Sirt Basin, vol. 1. Elsevier, Amsterdam, pp. 529–539.
Anketel, J.M., 1996. Structural history of the Sirt basin and its relationships to the Sabratah Basinand cyrenaican platform, northern Libya. In: Salem, M.J., El-Hawat, A.S., Sbeta, A.M. (Eds.), The Geology of Sirt Basin, vol. II. Elsevier, Amsterdam, pp. 57–87.
Ashour, M.M., 1996. Microbiostratigraphical analysis of the campanian–maastrichtian strata in some wells in Sirt basin. In: Salem, M.J., Busrewil, M.T., Misallati, A.A., Sbeta, M.A. (Eds.), The Geology of the Sirt Basin. Elsevier, Amsterdam, pp. 243–264.
Baird, D.W., Aburawi, R.M., Bailey, N.J.L., 1996. Geohistory and petroleum in the central Sirt basin. In: Salem, M.J., Busrewil, M.T., Misallati, A.A., Sola, M.A. (Eds.), The Geology of the Sirt Basin, vol. 3. Elsevier, Amsterdam, pp. 3–56.
Burwood, R., Redfern, J., Cope, M., 2003. Geochemical evaluation of East Sirte Basin (Libya) petroleum systems and oil provenance. In: Burnham, T., MacGregor, D.S., Cameron, N.R. (Eds.), Petroleum Geology of Africa. Geol. Soc. Lond., Spec. Publ., vol. 207, pp. 203–240. https://doi.org/10.1144/GSL.SP.2003.207.01.11.
Conant, L.C., Goudarzi, G.H., 1967. Stratigraphic and tectonic framework of Libya. Bull. Assoc. Pet. Geol. 51, 719–730.
Cornford, C., 1998. Source rocks and hydrocarbons generation and expulsion. In: Glennie, K. (Ed.), Petroleum Peology of the North Eea Basic Concepts and Recent Advances, fourth ed. Wiley-Blackwell, Oxford, pp. 376–462. https://doi.org/10.3896/IBRA.1.47.4.18.
Diasty, W.S., Beialy, S.Y., Peters, K.E., Atfy, H. El, Gheith, A.M., Agha, N.N., 2016. Organic geochemistry of crude oils and upper cretaceous source from concession 11, west Sirte Basin, Libya. J. Petrol. Geol. 39, 393–413.
El-Alami, M.A., 1996. Habitat of oil in Abu Attiffel area, Sirt basin, Libya. In: Salem, M.J., El-Hawat, A.S., Sbeta, A.M. (Eds.), First Symposium on the Sedimentary Basins of Libya, Geology of the Sirt Basin, vol. 2. Elsevier, Amsterdam, pp. 337–348.
El-Alami, M., Rahouma, S., Butt, A.A., 1989. Hydrocarbon habitat in the sirte basin northern Libya. Pet. Res. Journ. Tripoli 1, 17–28.
Ghori, K.A.R., Mohammed, R.A., 1996. The application of petroleum generation modelling to the eastern Sirt Basin, Libya. In: Salem, M.J., El-Hawat, A.S., Sbeta, A.M. (Eds.), First Symposium on the Sedimentary Basins of Libya, Geology of the Sirt Basin, vol. 2. Elsevier, Amsterdam, pp. 529–540.
Goudarzi, G.H., 1980. Structure–Libya. In: Salem, Busrewil, M.J. (Eds.), The Geology of Libya, vol. III. Academic Press, London, pp. 879–891.
Guiraud, R., Bosworth, W., 1997. Senonian basin inversion and rejuvenation of rifting in Africa and Arabia: synthesis and implications to plate-scale tectonics. Tectonophysics 282, 39–82.
Gumati, Y.D., Nairn, A.E.N., 1991. Tectonic subsidence of the sirte basin, Libya. J. Petrol. Geol. 14, 93–102.
Gumati, Y.D., Schamel, S., 1988. Thermal maturation history of the sirte basin, Libya. J. Pet.Geol. 11, 205–218.
Gumati, Y.D., Kanes, W.H., Schamel, S., 1996. An evaluation of the hydrocarbon potential of the sedimentary basins of Libya. J. Petrol. Geol. 19, 39–52.
Hallett, D., 2002. Petroleum Geology of Libya. Elsevier, Amsterdam, p. 503.
Hallett, D., 2016. Petroleum Geology of Libya. Elsevier, Amsterdam, Netherlands, p. 330.
Hallett, D., El Ghoul, A., 1996. Oil and gas potential of the deep trough areas in the Sirt Basin. In: Salem, M.J., El-Hawat, A.S., Sbeta, A.M. (Eds.), The Geology of Sirt Basin, vol. II. Elsevier, Amsterdam, pp. 455–482.
Harding, T.P., 1984. Graben hydrocarbon occurrences and structural style. Am. Assoc. Petrol. Geol. Bull. 68, 333–362.
Hassan, H.S., Kendall, C.C.G., 2014. Hydrocarbon provinces of Libya: a petroleum system study. In: Marlow, L., Kendall, C., Yose, L. (Eds.), Petroleum Systems of the Tethyan Region: AAPG Memoir 106, pp. 101–141. https://doi.org/10.1036/13431855M1063608.
Horsfield, B., 1994. Metagenesis of Organic Matter, vol. 60. AAPG Memoir, pp. 189–199.
Jawazi, A.F., Futyan, 1996. The hydrocarbon habitat of the oil and gas of north Africa with emphasis on the Sirt Basin. In: Salem, M.J., El-Hawat, A.S., Sbeta, A.M. (Eds.), The Geology of Sirt Basin. Elsevier, Amsterdam, pp. 287–308.
Klemme, H.D., 1994. Petroleum systems of the world involving upper Jurassic srource rocks. AAPG Memoir 60, 51–72.
Macgregor, D.S., Moody, R.T.J., 1998. Mesozoic and cenozoic petroleum systems of north Africa. Geol. Soc. Special publication No. 132. In: Macgregor, D.S., Moody, R. T.J., Clark- Lowes, D.D. (Eds.), Petroleum Geology of North Africa, pp. 201–216.
McKenzie, D., 1981. The variation of temperature with time and hydrocarbon maturation in sedimentary basins formed by extension. Earth Planet Sci. Lett. 55, 87–98. https://doi.org/10.1016/0012-821X(81)90089-3.
Megerisi, M., Mamgain, V.D., 1980. The upper cretaceous–tertiary formations of northern Libya. In: Salem, M.J., Busrewil, M.T. (Eds.), The Geology of Libya. Academic Press, London, pp. 67–72.
Nyblade, A.A., Suleiman, S., Roy, R.F., Pursell, B., Doser, D.I., Keller, G.R., 1996. Terrestrial heat flow in the Sirte Basin, Libya, and the pattern of heat flow across northern Africa. J. Geophys. Res. 101.
Pepper, A.S., Corvi, P.J., 1995. Simple kinetic models of petroleum formation: Part I. Oil and gas generation from kerogen. Mar. Petrol. Geol. 12, 291–319.
Robertson Research Group, 1989. Petroleum Geochemical Evaluation of the Western Sirt Basin, Libya. Project No. RGPD/889/Ic/25285, Prepared for Mobil Oil Libya.
Roohi, M., 1996a. A geological view of source–reservoir relationships in the western Sirt Basin. In: Salem, M.J., El-Hawat, A.S., Sbeta, A.M. (Eds.), Geology of the Sirt Basin, vol. 2. Elsevier, Amsterdam, pp. 323–336.
Roohi, M., 1996b. Geological history and hydrocarbon migration pattern of the central Az Zahrahe Al Hufrah platform. In: Salem, M.J., El-Hawat, A.S., Sbeta, A.M. (Eds.), Geology of the Sirt Basin, vol. 2. Elsevier, Amsterdam, pp. 435–454.
Rossi, M.E., Tonna, M., Larbash, M., 1991. Latest jurassic–early cretaceous deposits in the subsurface of the eastern Sirt basin (Libya). In: Salem, M.J., El-Hawat, A.S., Sbeta, A.M. (Eds.), The Geology of Sirt Basin, vol. 2. Elsevier, Amsterdam, pp. 2211–2225.
Rusk, D.C., 2001. Libya: petroleum potential of the underexplored basin centres–a twenty-frist century challenge. AAPG Mem 74, 429–452.
Sikander, A.H., Basu, S., 2000. Source-maturation, Structural Synthesis and Volumetric Estimates for Upper Cretaceous Source–Rocks, West Central Sirt Basin. Sirte Oil Company, Sirte-Libya.
Sikander, A.H., Basu, S., Wafa, F., 2006. Atlas of Petroleum Geology and Geochemistry of Mesozoic Source Rocks and Hydrocarbons in Sirt Basin, Libya, vol. 1. Libyan Petroleum Research Center, Sirte-Libya.
Ungerer, P., 1990. State of the art of research in kinetic modelling of oil formation and expulsion. In: Durand, B., Behar, F. (Eds.), Advances in Organic Geochemistry. Pergamon Press, Oxford, pp. 1–25.
Waples, D.W., 1994. Modeling of sedimentary basins and petroleum systems. In: Magoon, L.B., Dow, W.G. (Eds.), The Petroleum System from Source to Trap. AAPG Memoir 60, pp. 307–362.
Wennekers, J., Wallace, F., Abugares, Y., 1993. The geology and hydrocarbons of the Sirte Basin. In: Salem, M.J., El-Hawat, A.S., Sbeta, A.M. (Eds.), The Geology of Sirte Basin. Elsevier, Amsterdam, pp. 3–56.
Ziegler, P.A., Roure, F., 1999. Petroleum systems of Alpine–Mediterranean fold belts and basins. In: Durand, B., Jolivet, L., Horvath, F., Seranne, M. (Eds.), The Mediterranean Basins: Tertiary Extension within the Alpine Orogen. Geological Society, London, pp. 517–546.